Earthquake probabilities and probabilistic shaking in Italy in 50 years since 2003: trials and ideas for the 3rd generation of Italian seismic hazard maps

L. Peruzza

Istituto Nazionale di Oceanografia e Geofisica Sperimentale - OGS, Trieste, Italy

(Received March 27, 2006; accepted September 4, 2006)

ABSTRACT In the frame of the activities promoted by the National Group for the Defence against Earthquakes, a four-year national project has been funded on the topic of determining priorities in seismic risk mitigation at the national scale. This paper describes the efforts to introduce individual faults and time-dependent issues in the seismic hazard assessment developed within this project. The elaborations refer to the national scale and use some original data produced and released for the project's purposes, namely, the Database of Italy's Seismogenic Sources and a compilation of the Italian instrumental earthquakes from 1981 until 2002. An integrated seismic hazard model that combines the individual earthquake sources recognised by geological and seismological studies with the information obtained by the national seismographic network is proposed and applied to the seismic hazard assessment. Individual sources are assumed to follow the characteristic earthquake model and their rates of occurrence derived from geometric and kinematic considerations. The minor seismic activity defined in terms of background sources is represented by Gutenberg-Richter relationships calibrated on the instrumental dataset. Then, the conditional probability of occurrence of characteristic earthquakes for each individual source is modelled by the Brownian-Passage-Time distribution. The simple time-dependent hypotheses introduced are used to derive equivalent fictitious seismicity rates: they can be entered into traditional seismic hazard codes for having maps that are referred to the time when the analysis has been performed. The results are heavily controlled by some arbitrary choices like the regional distribution of slip rate (applied to all individual sources lacking detailed information), or the uncertainties a priori attributed to the mean recurrence time. Nevertheless, the maps of conditional probability of earthquake occurrence and the seismic hazard maps, under Poisson and time-dependent hypotheses, enhance the role of moderate earthquakes in driving the seismic hazard. The databases have been updated during the life of the project and the new versions became public after the project ended. The elaborations presented here refer to the data available during the project and were not updated to be consistent with the final products released by the project. The results obtained must therefore, be considered mainly for their methodological approach to the problem, so their application to seismic protection strategies has to be done with great care.

1. Introduction

Italy has two generations of seismic hazard maps. The first one (Gruppo di Lavoro Scuotibilità, 1979) belongs to the historical probabilisms (Muir Wood, 1993) with expected shaking, in terms of macroseismic intensity (MCS scale), computed on the earthquake catalogue (Postpischl, 1985) using Gumbel statistics. These maps are the basis of the first seismic zonation (Petrini *et al.*, 1980) adopted by the government in the '80s. The second generation represents the so-called seismotectonic probabilisms, with estimates in macroseismic intensity, peak ground acceleration (PGA) and spectral acceleration (SA) and computations related to a traditional Cornell-type approach (Bender and Perkins, 1987). Several maps have been realized and published in less than 10 years, from the original first version (Slejko *et al.*, 1998), through the elaborations that guided the proposal of updating the seismic zonation (Gruppo di Lavoro, 1999; Albarello *et al.*, 2000) introduced by law in 2003, to the most recent maps (Gruppo di Lavoro, 2004). All these results, using different levels of complexity and slightly different databases, share the philosophy of using polygonal sources, which gather individual faults and accept the assumption of stationarity of the seismic process, making the prediction insensitive to the time of the analysis.

During the last decade, the Italian scientific community has faced a difficult transition to a third generation of hazard maps, capable of addressing individual sources and introducing simple rules of time-dependency from the time of prediction. Worldwide, the consensus on this matter is generally poor and a few papers have been published for Italy (Peruzza *et al.*, 1997; Peruzza, 1999; Faenza *et al.*, 2003; Marzocchi *et al.*, 2003; Romeo, 2005). For many years in the Mediterranean countries, the problem of completeness of the historical catalogue has been approached independently of any reasoning about the velocity of the deformation, as the geological complexity often inhibits surface recognition of individual earthquake sources. Nowadays, in most of Italy this velocity has been shown to be from 1/10 to 1/100 smaller than those registered in other seismically active regions (California, or the Anatolian Range, for example) with associated mean recurrence times of big earthquakes longer than hundreds of years. In these cases, the identification of gaps that are potentially seismic and the introduction of the time elapsed since the last event may significantly alter the hazard estimates.

Other than seismic zoning purposes, seismic hazard maps using individual faults and time-dependent assumptions are critical for planning the priorities in allocation of resources devoted to retrofit the existing buildings and strengthen systems and infrastructures. On these topics, a four-year project named, "Probable earthquakes in Italy from year 2000 to 2030: guidelines for determining priorities in seismic risk mitigation" (Amato and Selvaggi, 2004) has been developed in the frame of the activities of the "Gruppo Nazionale per la Difesa dai Terremoti" (GNDT), promoted and financed by the National Civil Protection Department. The work presented here is one of the results obtained by this project; the final results released by this study may be found in the "Prodotto N.14" at the web site address http://gndt.ingv.it/Att_scient/Prodotti_consegnati/Amato_Selvaggi/prodotti_Amato.htm.

This paper aims to:

1) define a procedural scheme to assign earthquake occurrence rates to the individual sources proposed by other investigators. As observations do not permit a tight definition of the earthquake model throughout the country, the individual sources are modelled permitting they follow the characteristic earthquake model (Schwartz and Coppersmith, 1984). The largest event corresponds to the characteristic earthquake, while the low magnitude

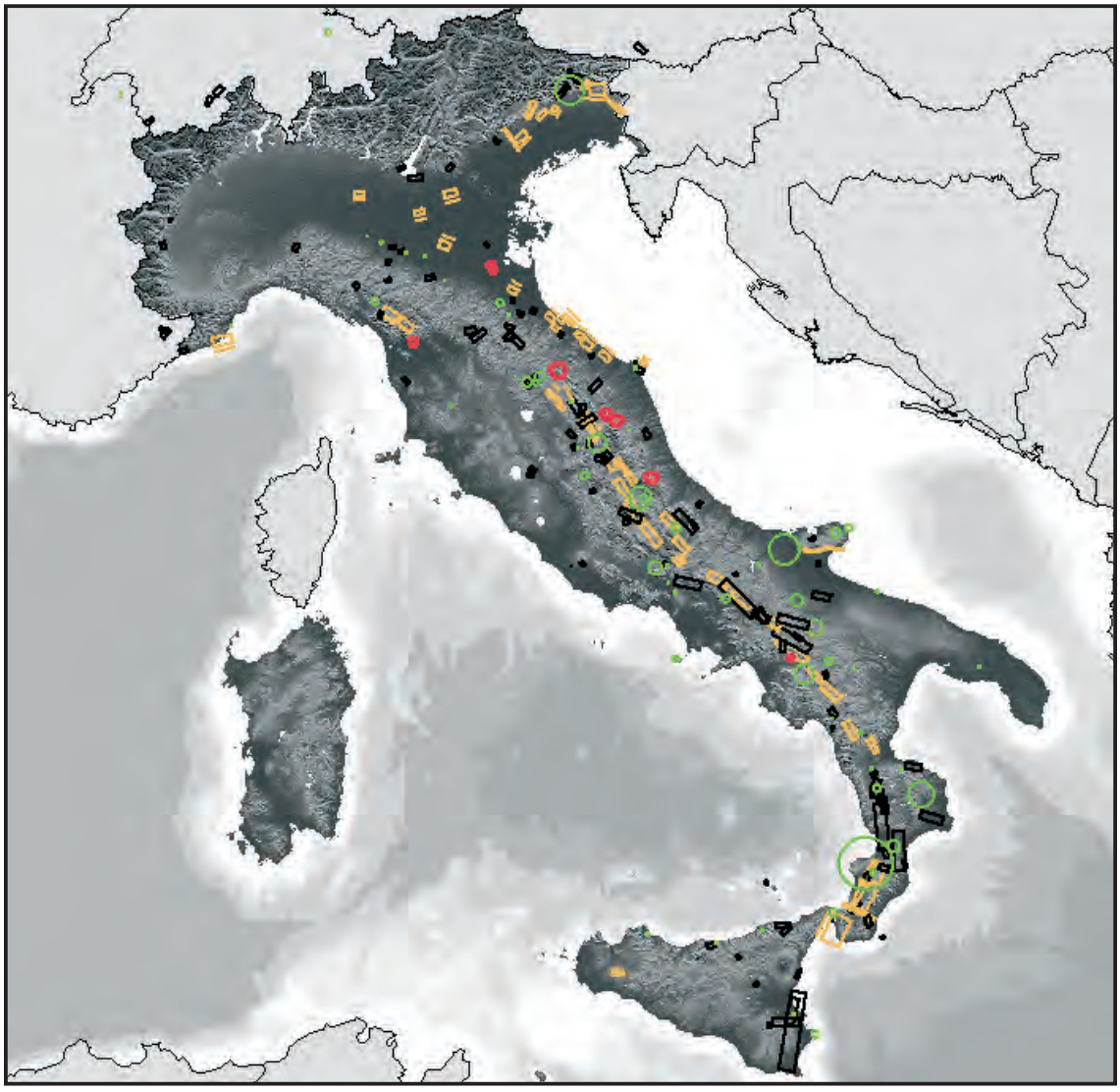

Fig. 1 - Database of Italy's Seismogenic Sources (DISS), version 2.0.516 released at the beginning of the GNDT project (Valensise and Pantosti, 2001): the integrated dataset addresses four kinds of sources: the geological ones (yellow rectangles), the historical well-constrained sources (black rectangles), the historical badly-constrained sources (green circles), the deep sources (red octagons).

earthquakes of the same region, referred to as "background seismicity", are calibrated independently on the instrumental earthquake catalogue for the last several years;

2) formalize, whenever possible, the uncertainties that enter into the seismogenic characterization;
3) introduce, in a simplified manner, memory into the estimates, adopting the renewal process model described by Brownian-Passage-Time (BPT) distributions;
4) compute some preliminary maps in terms of occurrence probability of earthquakes on individual structures and in terms of probabilistic expected shakings.

The final considerations are therefore oriented towards describing the sensitiveness of these studies on the selected models and parameters and give some suggestions for gathering, in Italy, data useful for these studies. As some strong simplifications and approximations have been introduced into the elaborations, the results must be considered a first, perfectible approach to the problem.

2. Individual sources

The individual sources used in this study are those gathered in the database commonly referred to as the Database of Italy's Seismogenic Sources (DISS). The first version 2.0.516 published in 2001 (Valensise and Pantosti, 2001), at the beginning of the GNDT project, has been used for the present analysis, following the authors' selection addressed like the dataset of the "integrated sources" (Fig. 1).

The 242 DISS sources are ranked in four categories, in relation to the available knowledge.

The first kind of sources collects the best-known structures quoted as "geologically constrained sources" (yellow boxes in Fig. 1). This fragmented collection of sources represents faults controlled by morphotectonic features, geological and geophysical evidence, integrated in many cases by a proposed earthquake association, and by paleoseismological data. There are 60 sources in this category, in the magnitude range [M_{est}, corresponding to M_w, see Valensise and Pantosti (2001) for further details] between 5.2 and 7.0 (Fig. 2a): the biggest event is the 1908 Messina earthquake, 10 sources have an estimate of slip-per-event given by direct observations or coseismic modelling, for 11 sources the long-term slip rate is given by individual data. The date of the last event is given for 46 sources.

The second kind of sources is classified as "historical well-constrained sources" (109 boxes marked by black rectangles in Fig. 1, magnitude distribution in Fig. 2b). Here, the dimensions of the individual source are derived from the magnitude of the earthquake, by empirical relationships (Wells and Coppersmith, 1994), the orientation of the box is controlled by the distribution of the maximum damage. No slip-per-event, or slip rate is provided and the date of the last event is always given, as each source uniquely corresponds to a record in the earthquake catalogue. The largest earthquake that belongs to this kind of source is the 1693 one in eastern Sicily.

Then, DISS defines 65 "historical badly-constrained sources" (green circles in Fig.1, magnitude distribution in Fig. 2c). They represent the location of the earthquake records reported in the catalogue: the dimension of the source (diameter of the circle) is again derived from magnitude, and similarly to the previous case, only the date of the event is provided. For these events, the distribution of the effects is poorly defined to fix the elongation of the source. The biggest event was the one offshore the Calabrian arc in 1905, but some very recent events, like the 1990 Augusta earthquake [Sicily, M=5.3, identification number (ID) of the source 724] have been assigned to this kind of source.

Finally, 8 so called "deep sources" are mapped (Fig. 1, red octagons, magnitude is plotted versus the year of the earthquake in Fig. 2d) and they refer to earthquakes that exhibited anomalously large perceptibility areas, suggesting a deep (more than 40 km) focus. Deep events deserve peculiar relationships to quantify the dimension of the source, as well as adequate attenuation relations for modelling the PGA; these sources will not be used in the following analyses as they are rare and scarcely contribute to the hazard.

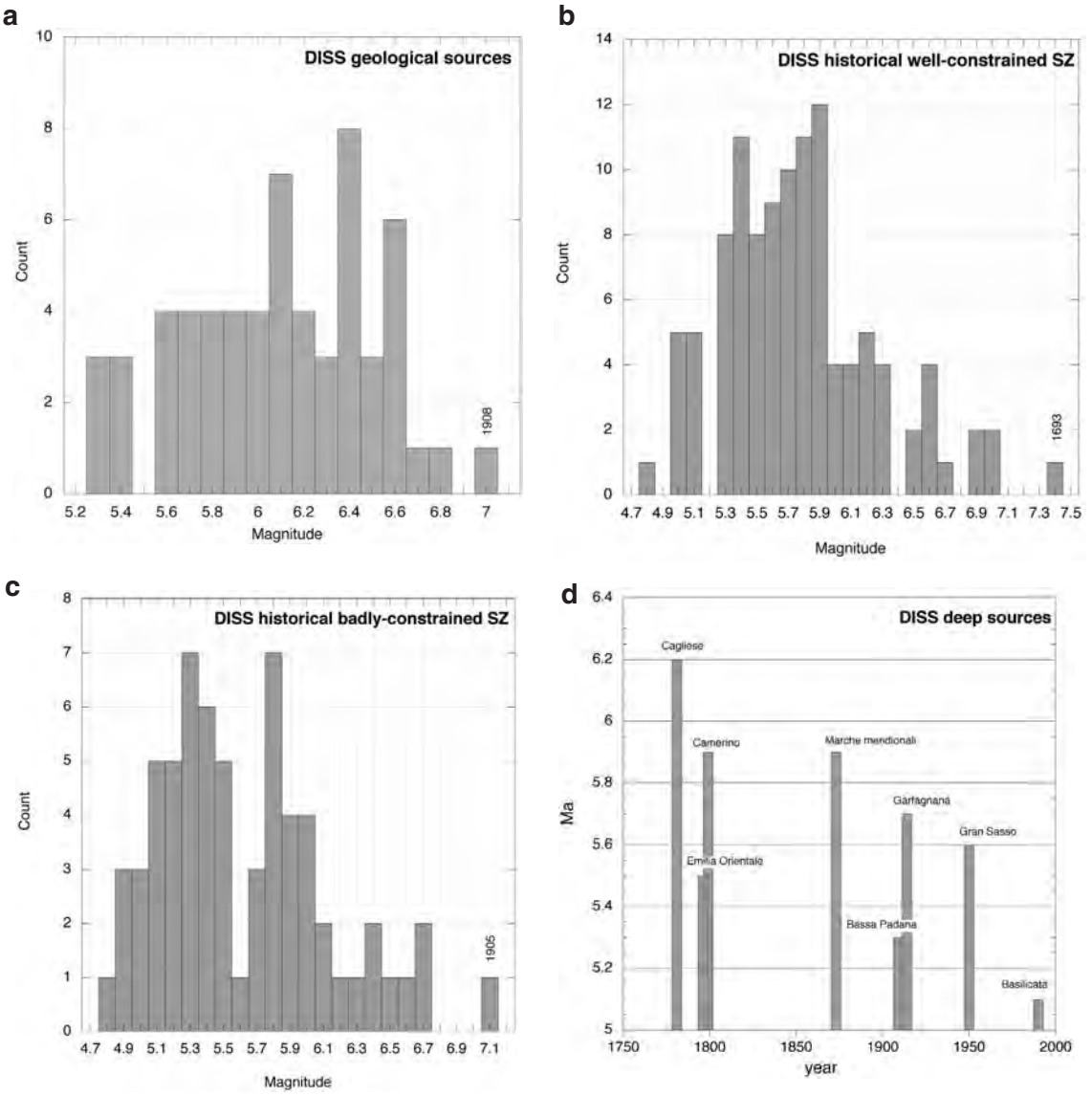

Fig. 2 - Magnitude distribution in the DISS sources: the magnitude type is equivalent to M_w, for the geological source only [see details in Valensise and Pantosti (2001)].

The geological and historical individual sources defined in DISS follow *"the basic assumption that each seismogenic source tends to generate repeatedly and exclusively its largest allowed earthquake, that is the assumption of "characteristic" behaviour [in the sense of Schwartz and Coppersmith (1984)] for what concerns fault location, geometry and size"* (Valensise and Pantosti, 2001, p. 802). Therefore, in this study the long-term seismic potential of a fault segment has been modelled by the spike, or more precisely by the simple bell of a Gaussian distribution (Fig. 3), corresponding to the largest allowed event stated by the characteristic earthquake model. All the M<5.5 events, not represented by individual seismogenic sources in DISS, would be modelled in

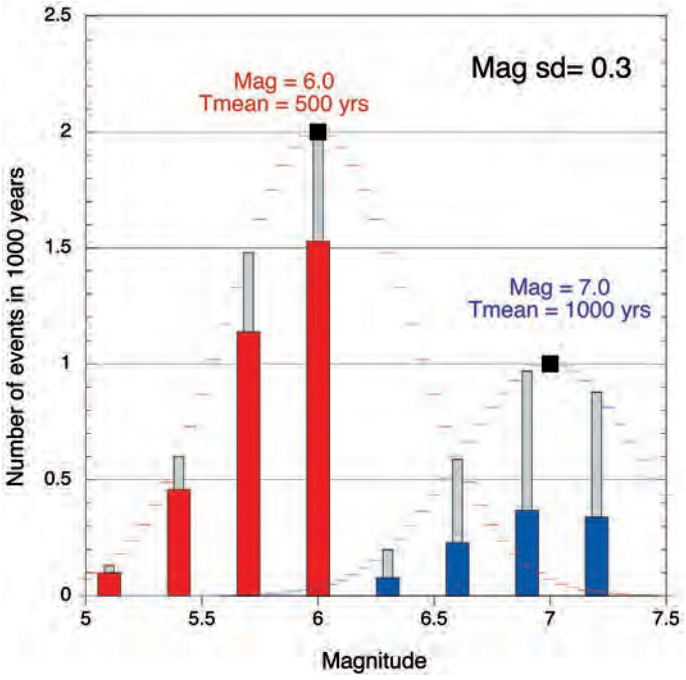

Fig. 3 - Gaussian model of a characteristic earthquake: a Gaussian distribution (coloured small traits) is anchored to the magnitude and recurrence time of a hypothetic characteristic event (black squares): the magnitude continuous function is sampled (step 0.3) in the interval $-3sd/+sd$ (grey bars), and then scaled (coloured bars) to preserve to total amount of seismic moment. These non-cumulative annual seismicity rates can be directly used in the seismic hazard code SEISRISK III (Bender and Perkins, 1987).

Table 1 - DISS geological sources: identification code (ID) and name.

ID	Name	ID	Name
1	Ovindoli-Pezza	32	Pesaro San Bartolo
2	Fucino Basin	33	Rimini offshore South
3	Aremogna-Cinque Miglia	34	Rimini offshore North
4	Boiano Basin	35	Rimini
5	Tammaro Basin	36	Val Marecchia
6	Ufita Valley	37	Gubbio South
7	Irpinia South	38	Gubbio Middle
8	Agri Valley	39	Gubbio North
9	Castrovillari	40	Aspromonte Northwest
10	Melandro-Pergola	41	Scilla offshore
11	Upper Mesima Basin	42	Aspromonte Northeast
12	Gioia Tauro Plain	43	Aspromonte East
13	Messina Straits	44	Nicotera-Rosarno
14	Belice	50	Garfagnana North
15	Montereale Basin	51	Garfagnana South
16	Norcia Basin	100	Bagnacavallo
17	Colfiorito North	101	Montello
18	Colfiorito South	102	Asolo
19	Sellano	103	Mantova
20	Monte Sant'Angelo	104	Orzinuovi
21	San Giovanni Rotondo	105	Adige Plain
22	San Marco Lamis	107	Mirandola
23	Mercure Basin	120	Gemona East
25	Campotosto	121	Gemona North
26	Amatrice	122	Gemona West
27	Sulmona Basin	123	Pordenone North
28	Barrea	124	Cansiglio
29	Conero offshore	125	Alpago
30	Senigallia	126	Cividale
31	Fano Ardizio	130	Imperia

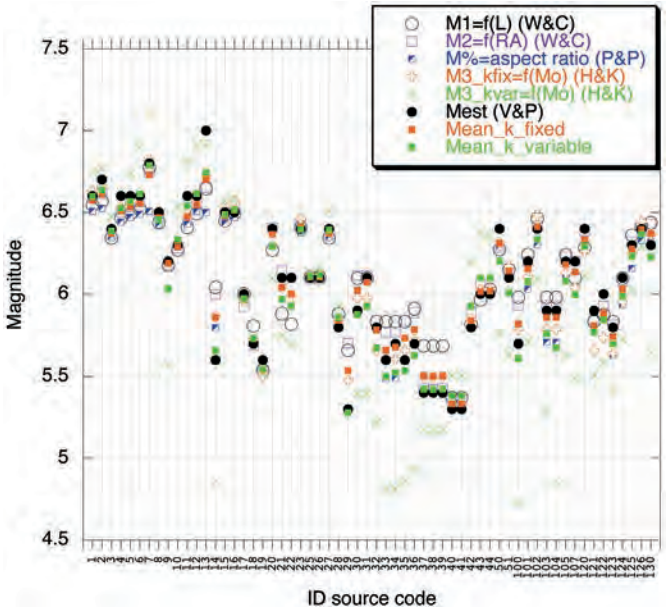

Fig. 4 - Magnitude values for the geological sources listed in Table 1: the black dot represents the values in DISS, while the others derive from relationships [description in the text, W&C stays for Wells and Coppersmith (1994), P&P for Peruzza and Pace (2002), H&K for Hanks and Kanamori (1979), and V&P for Valensise and Pantosti (2001)].

terms of "background seismicity". The validity of the characteristic earthquake idea is an intriguing question, widely criticized by authors objecting to the gap theory itself [see for example, Kagan and Jackson (1993)]. In the DISS' basic assumptions, it has been accepted in an even more simplistic formulation than the original one (Schwartz and Coppersmith, 1984; Youngs and Coppersmith, 1985), discarding the linear frequency-magnitude relation for smaller earthquakes, from which the large earthquakes deviate. Nevertheless, these simplifications may answer the fundamental question to *"focus on regions that have not released a large earthquake in the past millennium before attempting to explore it if there is any potential left within, or in the tails of, a historical rupture"* (Valensise and Pantosti, 2001, p. 803). They reflect, therefore, the wishful thinking of hazard analysts and follow important international experiences (e.g. Working Group on California Earthquake Probabilities, 1999).

The behaviour of each source is therefore assessed by the magnitude of the characteristic event (M_{max}) and its mean recurrence time (T_{mean}), assigning an estimate of the uncertainty on magnitude assessment given by the standard error of a Gaussian distribution, mainly for seismic hazard computational reasons. Given the occurrence model (Gaussian distribution of the seismicity rates) and its calibration point (M_{max}, $1/T_{mean}$), we can derive the earthquake occurrence rate of the individual sources in a straightforward manner and fix a seismic moment budget. The assumption of seismic moment conservation is necessary to assure that the total amount of seismic moment released by all the magnitude classes around M_{max} does not exceed the seismic moment released by the characteristic earthquake alone, whatever the magnitude-sampling factor of the Gaussian function is. Therefore, the total amount of seismic moment released by the sampled Gaussian

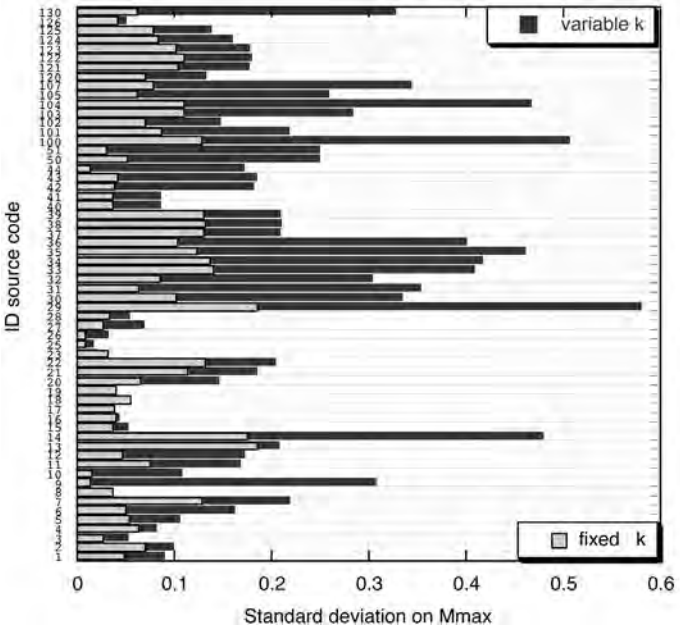

Fig. 5 - Uncertainties in the magnitude estimate of the characteristic event (M_{max}) for the geological sources: the light grey bar is the standard deviation under the assumption of constant strain drop (fixed *k*), the darker grey bar the *sd* using variable *k* assigned from the regional slip rate (in Fig. 11).

distribution (grey bars in Fig. 3, sample step of 0.3 in magnitude, commonly used in Italy in seismic hazard computations, as it roughly corresponds to a half degree in the macroseismic estimates) is made to equal the seismic moment released by the characteristic event (black squares in Fig. 3). This budgeting is done by fixing the seismic moment rate given by the maximum expected earthquake [i.e. $M_o(M_{max})$ in T_{mean} years] and by scaling the occurrences of each magnitude class properly; the sampling interval is not symmetric with respect to the M_{max} value (coloured bars in Fig. 3, where samples have been taken if the central value of the magnitude class M_{class} is $M_{max}-3sd \leq M_{class} < M_{max}+1sd$), as the higher magnitudes have a critical impact on the seismic moment release. The magnitude values M_{max} are always those given by the DISS compilers (M_{est}), but the way to obtain the other quantities (T_{mean}, uncertainties, and arbitrary choices done) differs for each kind of source, as described in the following.

2.1. Geological sources

The geological sources should be strictly controlled by independent observations: the dimension and shape of the box represent the surface projection of the segmented fault plane where repeated events are expected. In our case, the geometric parameters of the individual sources are often controlled by empirical regression relationships, only few cases of multiple events with dating are reported in the database DISS and they are not suitable for statistics. Consequently, and following previous experiences (e.g. Peruzza, 1999), M_{max} and T_{mean} have been obtained by regression relationships and compared with observations. M_{max} has been computed using empirical regression

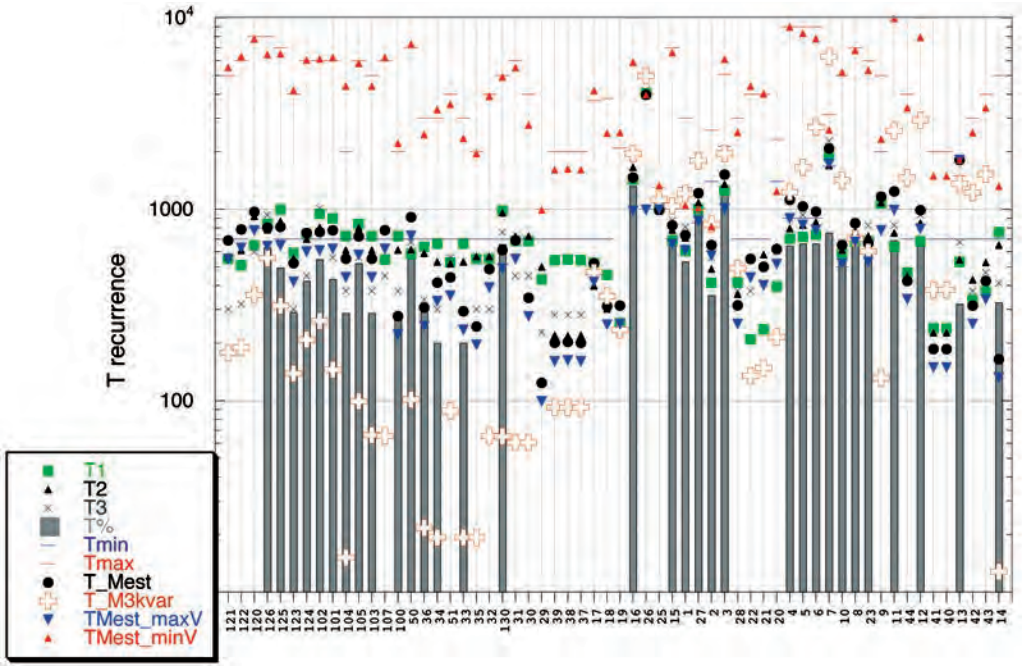

Fig. 6 - Recurrence times for the geological sources: T_{min} and T_{max} are the mean return times reported in DISS, the others derive from different choices of the magnitude or slip rate values (see text). For a better comprehension, the sources are sorted by latitude from north to south (see correspondence in Tab. 1).

relationships (Wells and Coppersmith, 1994) according to the style of the fault given by the rake values. In Fig. 4, *M*1 uses the surface length *L*, *M*2 the rupture area *RA* given by *LW*, where *W* is the down-dip length, and *M*3 uses the well-known relation M=2/3 [log(M_o) – 9.1] of the scalar seismic moment M_o [from Hanks and Kanamori (1979), M_o in Nm] given by:

$$M_o = \mu D L W = \mu k L^2 W \qquad (1)$$

where μ is the shear modulus fixed at $3x10^{10}$ Pa, D the average displacement-per-event, and k the strain drop. Two different hypotheses with constant and variable k values have been used: the constant k value is the value of $3x10^{-5}$ proposed by Selvaggi (1998), while variable trial k values have been derived from the zonation of the slip rate, as will be described in the following for the historical sources. A relationship based on aspect ratio considerations [i.e the ratio of W/L, see Peruzza and Pace (2002)] has also been applied to the set of geological sources [see the case study of central Italy in Pace *et al.* (2006)]. This suggests that if we consider the extension in depth of the seismogenic layer, the expected maximum magnitude (M% in Fig. 4) can be slightly reduced for some sources. All the values of M derived by regression relationships have been compared with the values (M_{est}) in DISS (Valensise and Pantosti, 2001) and some statistics have been performed on these values (Figs. 4 and 5). The computed values are somehow dispersed but the mean values (orange and green small squares in Fig. 4) are often coincident with the DISS values. This approach enables us to give a methodological way of estimating the uncertainties affecting the M_{max}

definition. Given a set of procedures that estimate the maximum magnitude of a fault segment, we may somehow characterize the uncertainty in the size of the characteristic event with a Gaussian function peaked on the mean magnitude value and as large as the related standard deviation is (Fig. 5). We may argue that not all the magnitude estimates are independent. Nevertheless, this choice surrogates the much more preferable situation of having a statistically relevant set of repeated observed magnitudes associated to the fault.

As the geometry of the geological sources identified in DISS is strictly controlled by empirical regression relationships, we obtain a dispersion on magnitude values that is much smaller than those actually observed. An enlightening example is the case of the Fucino Basin source (ID n. 2), whose computed magnitude values are all very close to the DISS values (M_{est}=6.8); the magnitude measured in 1915 is M_s=7.0 with a standard deviation *sd*=0.7 obtained on 22 observations (Margottini *et al.*, 1993). The observed value is fully compatible with M_{est} considering the M_w-M_s conversion and the computed standard deviation (see in Fig. 5), but the experimental uncertainty is, instead, much higher than what was hypothesized.

These considerations suggest that the calibration of uncertainties on the characteristic event magnitude of each individual source is, at this stage, more speculative than effective. I, therefore, decided to arbitrarily fix the narrowness of the peak of the Gaussian function to the standard deviation value of 0.3 for all the geological sources. It represents a cautious and reasonable value for the best defined sources. A higher value of 0.5 will be assigned to the historical sources on the basis of reasoning about the quality of magnitude assessment from macroseismic data (e.g. Stucchi and Albini, 2000).

Similar thoughts may be applied to define the mean return time associated with the characteristic event. The actual observations of multiple, similar-sized events on the same fault segment are few and limited to central Italy [see also Pace *et al.* (2006)]. Therefore, the T_{mean} associated with the maximum event was computed using the technique known as the conservation of the seismic moment rate on the fault segment (Field *et al.*, 1999):

$$1/T = \text{Char\_Rate} = \mu V L W / 10^{(1.5M+9.05)} \qquad (2)$$

where T is the mean return time, Char_rate the annual mean rate of occurrence, μ is the shear modulus, V the long-term slip rate, L and W the geometrical parameters of the fault. Considering different manners, the magnitude values and slip rate uncertainties given in DISS, the variability in T_s is reported in Fig. 6. Small fluctuations in the estimated M values cause large differences in the expected T_s, even if the V value is fixed (the return times referred to $M1$, $M2$, $M3$, $M\%$, M_{est} are all computed using the mean of the slip rate values given in DISS). Much worse is the effect of the uncertainties on the slip rate (the coloured triangles in Fig. 6 derive from fixed M_{est} values, and minimum and maximum slip rate assigned to each source). As most of the sources have been characterized by a regional "reasonable" slip rate varying from 0.1 to 1.0 mm/yr, the recurrence times may vary from hundreds to thousands of years as well. Therefore, I computed the mean and median values of these return times, by excluding the outliers (mean1, median1 in Fig. 7), or by using all the T_s (mean2 and median2, again in Fig. 7). Further elaborations will adopt the median1 values, as they are the nearest, on average, to the ones that use the magnitude values suggested by the DISS compilers (T_{Mest}), in combination with the mean slip rate. Again, statistics on these

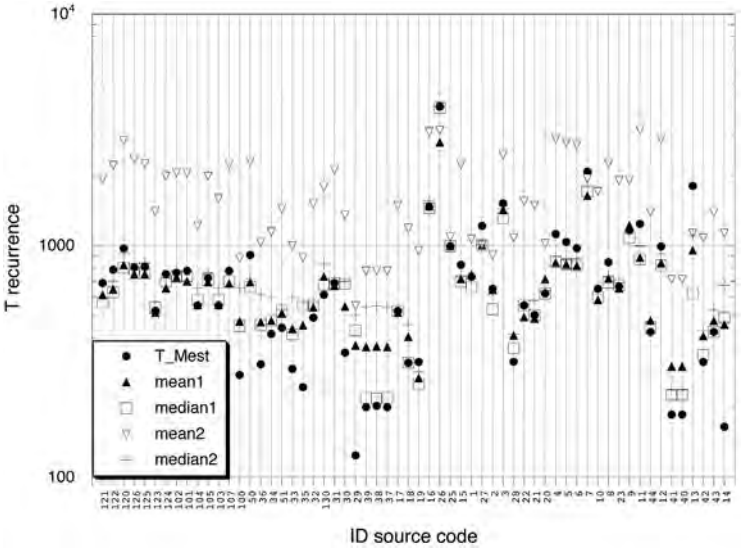

Fig. 7 - Statistics on the recurrence times of Fig. 6: T_{Mest} is the value obtained by Eq. (2), using the magnitude given in the DISS (M_{est}) and a mean value for the slip rate: mean1 and median1 refer to the statistics excluding the outliers, mean2 and median2 with all the T values. Sources are sorted as in Fig. 6 (see correspondence in Table 1).

fictitious recurrence times permits one to provide a simplistic answer to another critical parameter, concerning the uncertainties of inter-event times, necessary for modelling the distribution function of a renewal process. The α parameter of the BPT distribution is given by the ratio of standard deviation of the recurrence times over the mean recurrence time:

$$\alpha = \sigma / \mu.$$

It represents the aperiodicity of the distribution function [see Matthews *et al.* (2002) for further details] and is a key element for modelling the time-dependent processes. Here, it derives directly from the variance of the recurrence times. In Fig. 8, it has been computed and plotted for the DISS geological sources. It is evident that considering the whole uncertainty affecting the recurrence times (grey symbols in Fig. 8, derived from the statistics on all the times, mean2 and median2 in Fig. 7), the α values are much higher than the unit; discarding the outliers from the statistics (mean1 and median1 in Fig. 7, and corresponding α values with black dots in Fig. 8), most of the sources exhibit α's lower than 1/4, thus representing quasi-periodic processes consistent with the assumptions of the characteristic earthquake model, adopted a priori by the DISS.

Then, to summarize, the geological sources used here for the seismic hazard computations utilize their own geometry; the seismicity rate follows the characteristic earthquake model, controlled by geometric and kinematic indicators, using Gaussian distributions peaked on (M_{est}, Char_rate=$1/T_{median1}$) pair values and with a fixed, a priori given, standard deviation *sd* of 0.3. The continuous Gaussian function is sampled according to the magnitude step used by similar studies and is finally scaled to preserve the total amount of seismic moment released by the characteristic quake.

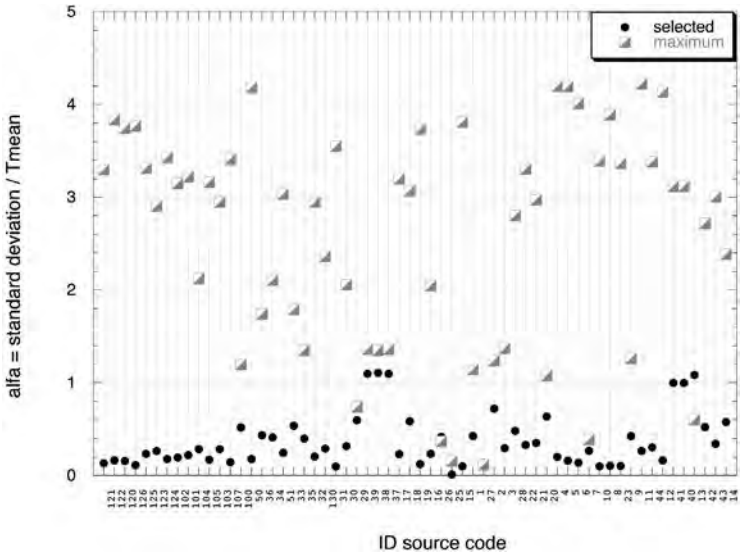

Fig. 8 - Uncertainties on the computed recurrence times for geological sources: the α value follows the formulation proposed by Matthews *et al.* (2002). Black dots refer to the set of recurrence times excluding the outliers (mean1 and median1 in Fig. 7): grey symbols for all the times graphed in Fig. 6.

The magnitude and recurrence time of the maximum expected event are, by far, the less constrained parameters available, but they are necessary in seismic hazard assessment. Only joint geological and seismological data can help constrain the model of long recurrences of maximum events.

2.2. Historical well-constrained and badly-constrained sources

The so-called historical sources are all the records of the earthquake catalogue without additional information. With variable degrees of uncertainty, the occurrence of the earthquake in the past constitutes the basis to infer the existence of a seismogenic structure in the area. Because the earthquake is not associated with a geological signature, the possible dimensions of the source derive exclusively from magnitude-based regression relationships. The geometries of historical well-constrained sources are forced by accepting the strong and questionable assumptions that link the elongation of the fault on the distribution of the maximum damage. The geological style at the regional scale permits us to derive an approximate down-dip length of the rupture (*W* values), and therefore, the thickness of the box. Badly-constrained historical sources have too few intensity data points even for such an approximation and circular sources are provided with the radius directly derived from the magnitude value.

There is no reason, therefore, to re-compute energetic parameters (*M*1 to *M*%) from the geometric characteristics of the segment, as done previously in Fig. 4. Only the M_{est} values can be considered. Similarly, the mean recurrence time of the fault cannot be, even tentatively, computed using Eq. (2), as neither the well-constrained nor the badly-constrained historical sources have original geometries and slip rate values given in the DISS.

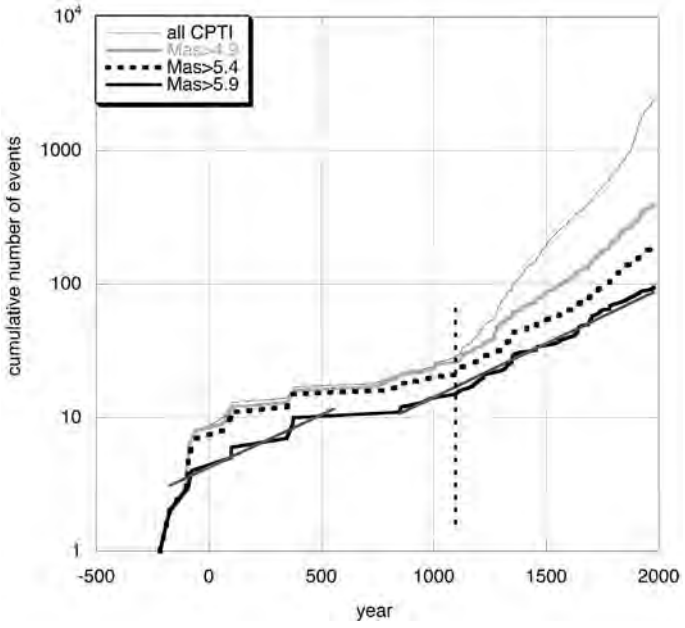

Fig. 9 - Catalogue of the Italian earthquakes CPTI04: graph of the cumulative number of events with increasing magnitude threshold [see the Mas definition in Working Group CPTI (2004)].

To obtain a trial spatial differentiation of the slip rate to characterize each individual source for the whole country, I decided to derive the long-term slip rate as a function of the seismic moment released by earthquakes. I used the parametric catalogue (Working Group CPTI, 2004) to obtain a very rough distribution of the seismic moment, simplistically converted into slip rate values. These values represent a first approximation of the strain balance problem, a field where only the availability of geodetic data can impose additional boundary conditions, fixing some problems that are not solved by the limited-in-time earthquake series.

The procedure to obtain a long-term slip rate from an earthquake catalogue is quite simple. Let an earthquake with magnitude M be occurred. If we define A an arbitrarily- shaped area pertaining to the source dimension, writing

$$L = f(A) = \sqrt{(A)} = c\sqrt{(R^2)}, \tag{3}$$

where R is an equivalent arbitrary radius and c the square root of π, and

$$W = f(L) = b\ c\ \sqrt{(R^2)} = b\ c R, \tag{4}$$

with simple mathematical transformations we can demonstrate that the seismic moment density (seismic moment per unit area) is independent of the geometric characteristics of the source L and W and it depends only on the displacement D and aspect ratio $b = W/L$ as follows:

$$M_o / \pi R^2 = \mu D A / \pi R^2 = \mu D L W / \pi R^2 = \mu D b. \tag{5}$$

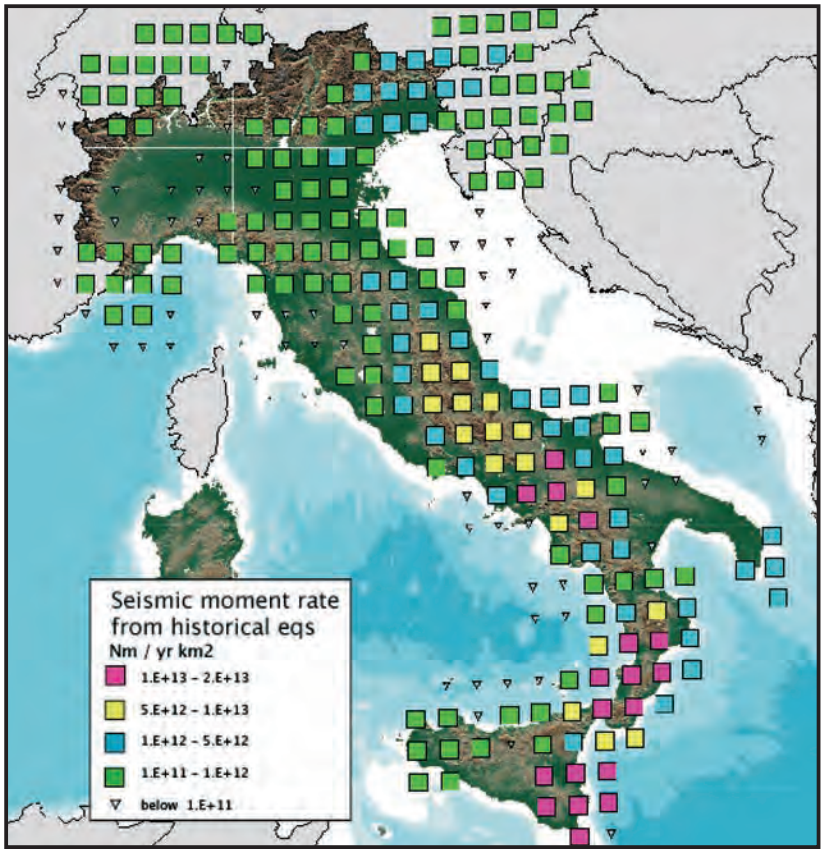

Fig. 10 - Annual seismic moment rate (Nm/yr ·km^2): computations have been made using M>5.5 events from 1100 to 2002, in a 60 km distance from the represented nodes.

If we indicate with T the mean return time associated to a source of characteristic earthquake, the slip rate of that fault can be written as:

$$V = D/T = M_o / \pi R^2 \mu b T. \quad (6)$$

Given many earthquakes insisting over an area S in a given time window Δt, the summation of their seismic moment may be interpreted using the seismic moment density and Eqs. (5) and (6) in terms of $\Sigma D_i/\Delta t$, which would represent the regional long-term slip rate, if the seismic records are considered complete and representative of the whole seismic cycle, and if the shear modulus μ and aspect ratio b are accepted to be constant over the area.

As a first approximation, viable at the national scale of the analysis, the completeness of the earthquake catalogue was estimated using simple graphical methods: plotting the cumulative number of events versus time, for the whole catalogue and for given thresholds of magnitude (Fig. 9). The graph demonstrates that the cumulative number of events exhibits a less or more pronounced break in the slope after the year 1000 and a significant increase in the slope after 1900, if all the

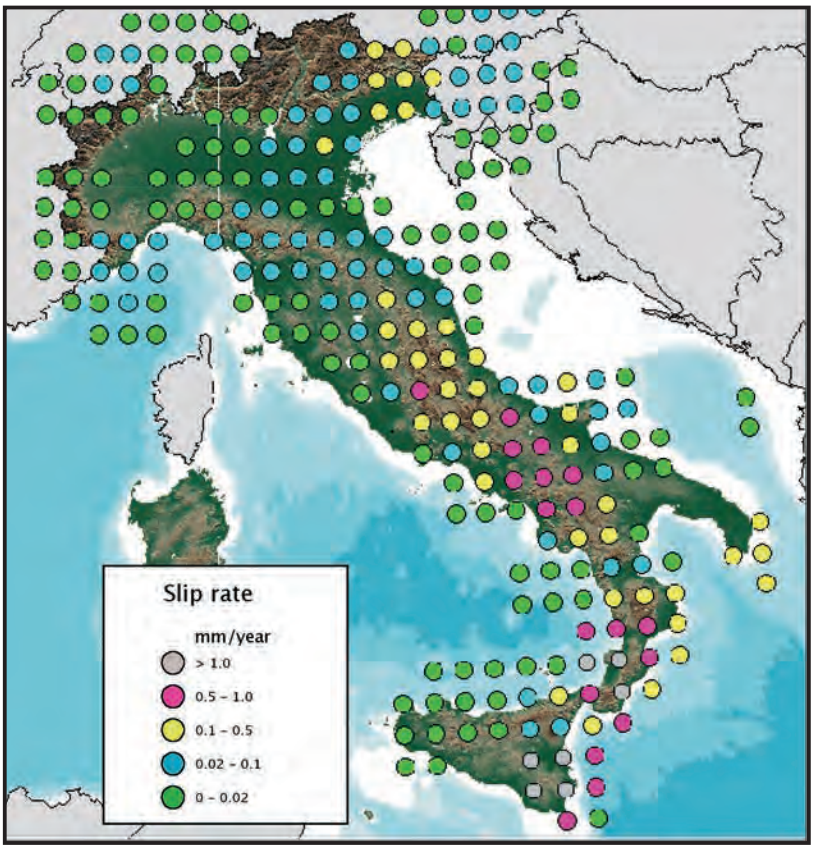

Fig. 11 - Lateral variation of slip rate (mm/yr) derived from the earthquake catalogue (annual seismic moment rate computed in Fig. 10, see description in the text).

events are included (thin line). Considering that:

a) the slope of the high magnitude threshold ($M \geq 6.0$, black thick curve) in Fig. 9 after the year 1100 is very similar to that referring to $M \geq 5.5$ (dotted curve);
b) the seismic moment release is dominated by the strongest events, and it decreases exponentially when the magnitude diminishes;
c) the CPTI catalogue is filtered for aftershocks, that are often responsible for an important budget in the total seismic moment released by a sequence;
d) the DISS database is, in theory, restricted to representative sources with $M > 5.5$;

a completeness for $M > 5.5$ from the year 1100 onwards is a reasonable assumption valid at the national scale [see for example Stucchi and Albini (2000) on that subject]. The working file released for the project's purposes [preliminary version of Working Group CPTI (2004)] has been integrated in the period 1993-2002 with the instrumental location with $M > 5.5$ and depth <50 km, compiled for the same project too (Chiarabba, 2003). The computation of the seismic moment rate has been done on a grid where the nodes are spaced 0.5 degrees in longitude and 0.4 in latitude, considering the epicentres are located inside a 60-km distance from the node. These search values were selected

after some tests, as having a smoothing effect on the seismic moment release that is compatible with the finiteness of the sources and with uncertainties in the locations. The seismic moment rate distribution mapped in Fig. 10 refers to a year and an arbitrary area of 1 km^2. The corresponding regional slip rate, mapped in Fig. 11, derives from Eq. (6), with μ = 3x10^{10} Pa, and b = 1/2; I therefore accept that no lateral variation of the shear modulus can be reasonably assessed and that the aspect ratio b is invariant to the size and the style of the event. The utilization of the rupture width given as a half of the rupture length is a very questionable condition, but it represents quite a cautious condition for moderate-to-strong events. Surprisingly, the values obtained are in good agreement with the few experimental long-term slip rate values, even if some lateral variations of the slip rate can reasonably be ascribed to incompleteness of the seismological catalogue: the most evident case can be seen in the northernmost part of Calabria, where no events are located by CPTI, but paleo-earthquakes have been recognised through trenches (e.g. Michetti *et al.*, 1997).

The seismic moment rate distribution of Fig. 10 has also been used to infer strain drop values by applying Eq. (5): laterally variable k's referred to a length of 1 km have been, therefore, assigned to the geological sources and used for an alternative computation of the magnitude associated to the sources. I am conscious that the lack of events in the earthquake catalogue introduces a systematic bias to the amount of the seismic moment release that propagates to the estimated mean recurrence times assigned to the source. A joint table of discussion, with seismologists, geologists and geodesists may likely aid in bridging this gap.

However, the slip rate values obtained from the earthquake catalogue have been assigned to the DISS historical sources (Fig. 12a), and a mean recurrence time for each source has been computed (Fig. 12b) by the ratio $T_{hist} = D/V$ (displacement over slip rate) where the displacement derives from empirical undifferentiated relationship (Wells and Coppersmith, 1994). The magnitude used is that given in the DISS with M_a and it represents a mean value between different estimates (instrumental if available, and derived from macroseismic data).

Similarly to the geological sources, historical sources may be used in the seismic hazard computations like characteristic event sources having their own geometry, and seismicity rate given by a Gaussian distribution. It is anchored to the (M_a, T_{hist}) values and a fixed, standard deviation of 0.5 is assigned a priori: this value is higher than that adopted for the geological sources, considering that only seismological data (mostly derived from macroseismic data) constrain the historical sources. As no estimate on the uncertainties of mean recurrence time is available, it has been assigned a provisional generic value of α= 0.5 for the historical well-constrained sources, similarly to what is usually done in literature (e.g. Ellsworth *et al.*, 1999; Romeo, 2005). The α value of the BPT distribution for the badly-constrained source is set to 1.0, corresponding to the characteristics of poor periodic processes. These choices will cause a very different behaviour in modelling the renewal process, as described in Matthews *et al.* (2002). α is one of the most challenging factors affecting the earthquake probabilities estimate, inducing a variability that may be of the same order, or even greater than the result, but unfortunately, no alternative solution has been provided.

For a simpler use in the seismic hazard codes and homogeneity reasons, I modified the geometry assigned to the badly-constrained historic sources. Instead of using circular sources, as in the DISS having the radius $R = f(M_a)$ (Wells and Coppersmith, 1994), I have modelled square sources, centred on the epicentral coordinates with latus $L = \sqrt{RA(M_a)}$, where the rupture area always derives from Wells and Coppersmith (1994) relationships (Fig. 13). This choice slightly enhances the

Fig. 12 - Slip rate in mm/yr (a) and mean recurrence time in years (b) associated to the historical sources of the DISS.

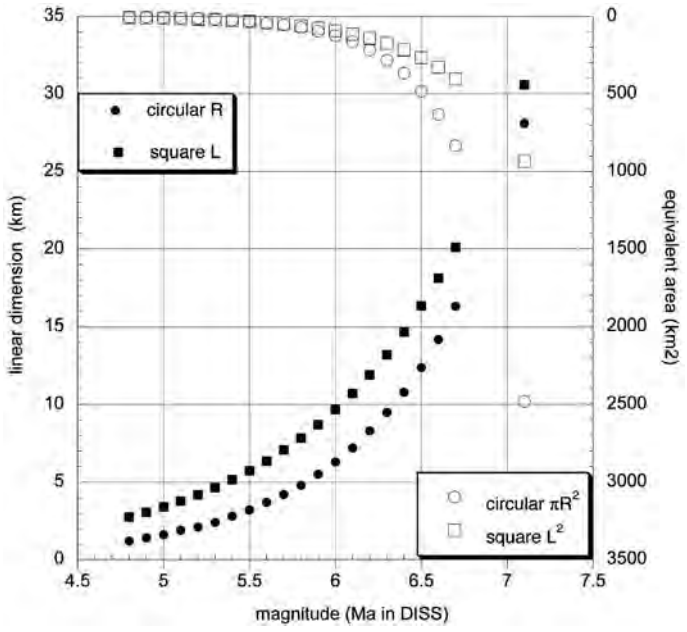

Fig. 13 - Correction on source dimension proposed for badly-constrained historical sources: L is the latus of the square source having rupture area $\log(RA)= -3.49+0.91 \cdot M$; R is the radius of the circular source proposed in the DISS, and derive from the subsurface rupture length relationship $\log(R)=-2.44+0.59 \cdot M$ (Wells and Coppersmith, 1994); on the right y-axis, the area associated to the source is plotted.

seismicity rates associated with the source, for the decrease of the area associated with the source (L^2, instead of πR^2), and is fully compatible with the procedures adopted for other individual sources.

3. Background sources

All earthquakes that cannot be referred to the individual sources will be treated in terms of background seismicity. I include in this category the low-level and diffuse seismicity that cannot be modelled by individual sources and the remnant low-magnitude queue of earthquakes invoked by the original formulation of the characteristic earthquake model (Schwartz and Coppersmith, 1984; Youngs and Coppersmith, 1985).

A basic assumption has been accepted for this kind of seismicity, i.e. that background seismicity is a stationary process that can be modelled by a Gutenberg-Richter (G-R) distribution. Therefore, the a and b values of the G-R relation are not supposed to vary with time. To calibrate these coefficients, the following procedure has been used.

The instrumental earthquake catalogue [preliminary version by Chiarabba (2003), published with some modifications in Castello *et al.* (2005)] has been taken as a sufficiently complete and reliable dataset for the entire country with the magnitude range of interest (M<5.5). The magnitude distribution provided in Fig. 14 suggests that below M=2.5, the dataset may be strongly affected by incompleteness. The G-R fitting on the whole dataset (cumulative number of events, small circles

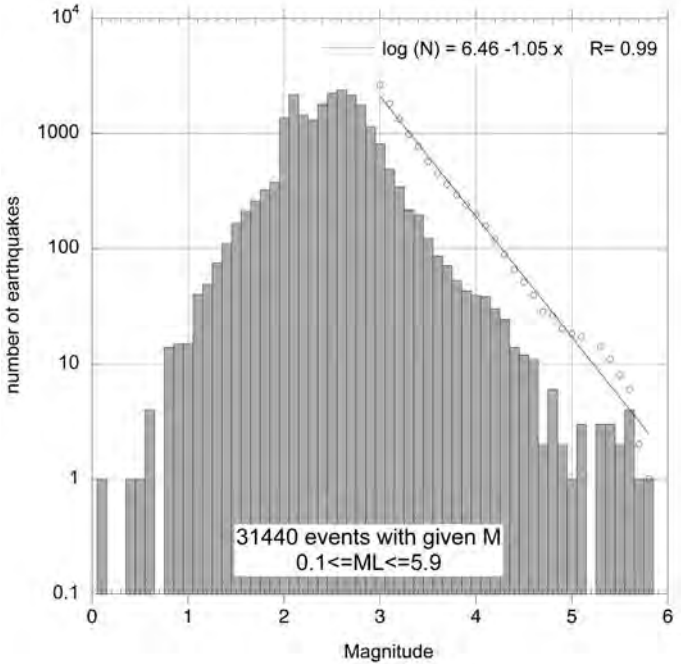

Fig. 14 - Magnitude distribution of events in the period 1981-2002, taken from the working catalogue of instrumental Italian earthquakes released for the project (Chiarabba, 2003): bars indicate the number of events in 0.1 magnitude classes, circles are the cumulative numbers interpolated by a G-R relationship (line) for $M \geq 3.0$.

in Fig. 14), suggests a *b*-value near the unit, with a pronounced bulge for $5.0 < M < 5.7$. The events that do have both magnitude and epicentral coordinates (28,780 located earthquakes) have been filtered to extract a list of independent events by using a modification of the procedure proposed by Knopoff (2000) - see also the comments reported in Pace *et al.* (2006). All quakes deeper than 50 km have been removed, as they slightly influence the seismic hazard.

Then, *a* and *b* values of the G-R relation have been computed, using a grid of 0.5° in longitude, 0.4° in latitude, with a search radius of 20 km. The traditional algorithms of least squares (lsq) and maximum likelihood (mlk) (Aki, 1965; Utsu, 1965, 1966; Weichert, 1980) have been used on the subsets having at least 3 events. The results obtained are mapped in Figs. 15 and 16 (*b* values, with both interpolation techniques, and *a* values, with lsq method, normalized to 1 year, considering the 22 years of the instrumental catalogue).

The *b* values (Fig. 15) show a very pronounced lateral variation, while the fitting algorithms have only a moderate influence on the results. After checking the interpolation of some nodes, the lsq method was chosen because it better fits the highest magnitude detected, although it is not formally correct. Nevertheless, the magnitude threshold of completeness in time and space is a delicate subject whose investigation is out of the scope of this paper. Some anomalous *a* and *b* values can be discarded simply by elevating the threshold of detected events from 3 to 5: the 206 nodes mapped in Figs. 15a and 16 are reduced to 169 and they have only been used to characterize the seismicity rates of rectangular cell sources of background seismicity. As the DISS database reports all instrumental events in the magnitude range 5.0-5.5 (see Fig. 2), the *a* and *b* values have been used to compute the

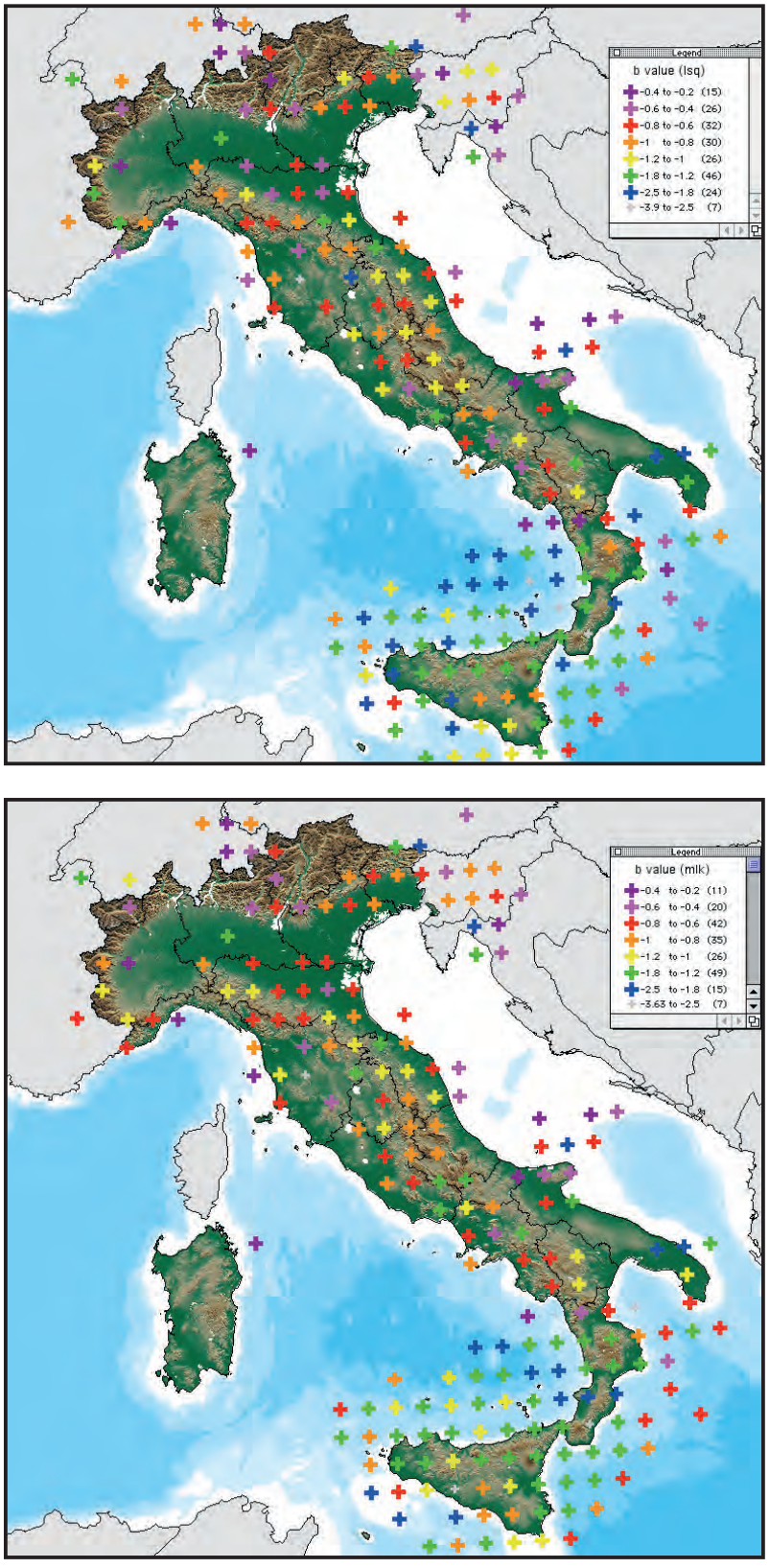

Fig. 15 - Distribution of *b*-values of the G-R relation, obtained from the instrumental catalogue, filtered from aftershocks: the interpolation has been done using lsq (a) and mlk (b) methods on the subset of events located in a 20 - km distance from the represented node.

Fig. 16 - Distribution of *a*-values of the G-R relation, computed as in Fig. 15a on subset of at least 3 events: the *a*-values are normalized to the period of one year. Only the nodes marked with bold symbols, having at least 5 events, have been used for further seismic hazard computations.

annual occurrences of earthquakes only for magnitude below 5.0, to avoid the same events (the Umbria-Marche sequence of 1997-98, for instance) being counted twice. The contribution of these cell sources to the global seismic hazard is significant, as will be shown later on.

4. Earthquake probabilities

The first application of the previous analyses is the computation of the probability of occurrence of a characteristic earthquake, in a given time period.

A rough estimate of probability of having a M_{max} event in the next years, conditional to the time elapsed since the last event, is given by the approaches proposed in Peruzza *et al.* (1997), Peruzza (1999), and Peruzza and Pace (2002). More recently, some papers (Sornette and Knopoff, 1997; Working Group on California Earthquake Probabilities, 2003; Pace *et al*. 2006) criticized the use of lognormal and gamma distributions as they are scarcely representative of the physical process of recharge of a fault, and the BPT distribution has appeared in seismological literature like the most physically motivated model (Ellsworth *et al.,* 1999; Matthews *et al.,* 2002).

Using the BPT formulation, the probability of an earthquake conditional to the time elapsed

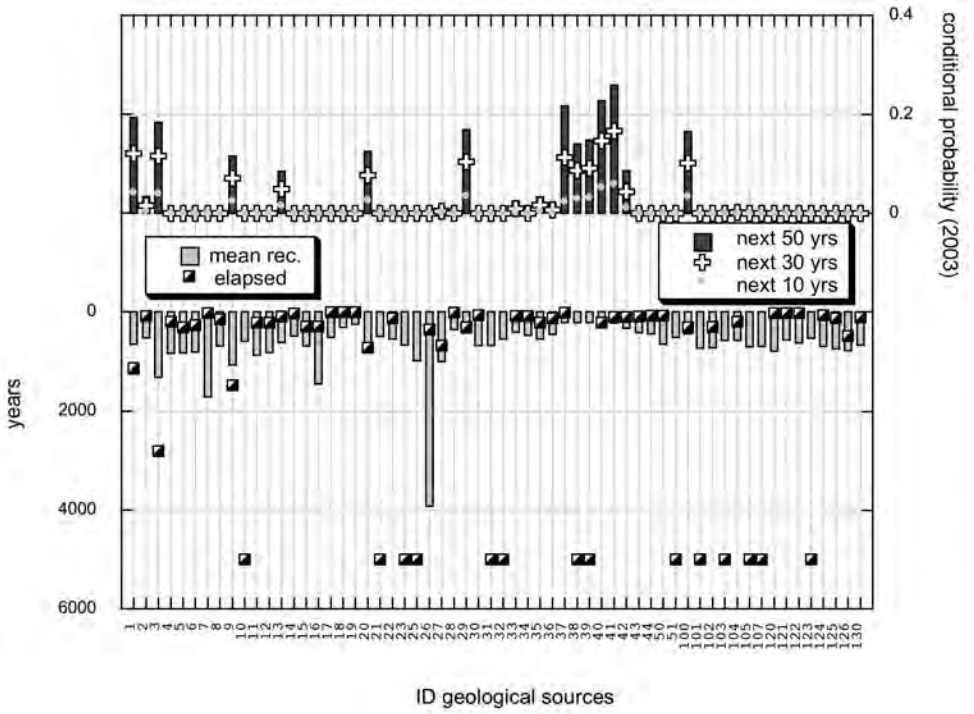

Fig. 17 - Renewal process modelled for DISS geological sources: conditional probability in different time intervals from 2003 (legend and y-axis on the right), given the mean recurrence (grey bars) and elapsed time (black and white squares) reported in the lower part of the graph (left y-axis): the α (aperiodicity) values are different for each source (selected values in Fig. 8): the date of the last event when not available is fixed at 3000 B.C. Most of the sources exhibit a negligible probability.

since the last event (T_e) can be calculated from the equations:

$$P(t \le T \le t + \Delta T) = \int_{t}^{t+\Delta T} \left(\frac{\mu}{2\pi\alpha^2 u^3} \right)^{1/2} \exp\left(-\frac{(u-\mu)^2}{2\alpha^2 \mu u} \right) du \tag{7}$$

$$P(Te \le T \le Te + \Delta T / T > Te) = \frac{P(Te \le T \le Te + \Delta T)}{1 - P(0 \le T \le Te)} \tag{8}$$

where μ is the mean recurrence time and α is a dimensionless measure of aperiodicity given by the ratio of standard deviation of the recurrence times over the mean recurrence time. Figs. 17 to 19 show the conditional probabilities of occurrences (from 2003) for the three kinds of sources reported in the DISS database. The computation of the conditional probability of occurrences has been done for three observation periods (10, 30, and 50 years): the differences have been represented for the geological source only in Fig. 17. Some geological sources do not have a date

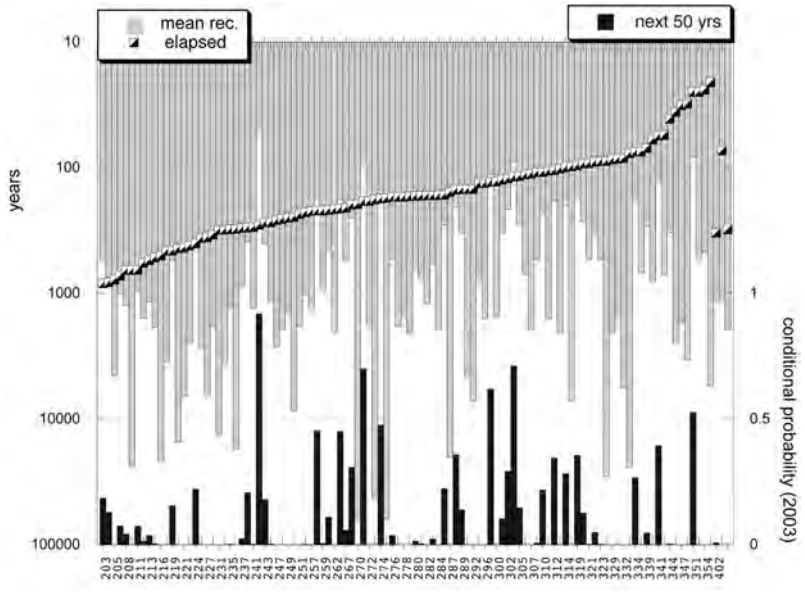

Fig. 18 - Renewal process modelled for DISS historical well-constrained sources: conditional probability in the next 50 years from 2003 (black bars, right y-axis), given the mean recurrence (grey bars) and elapsed time (squares) reported in the upper part of the graph (left y-axis): the α value is fixed, a priori, equal to 1/2.

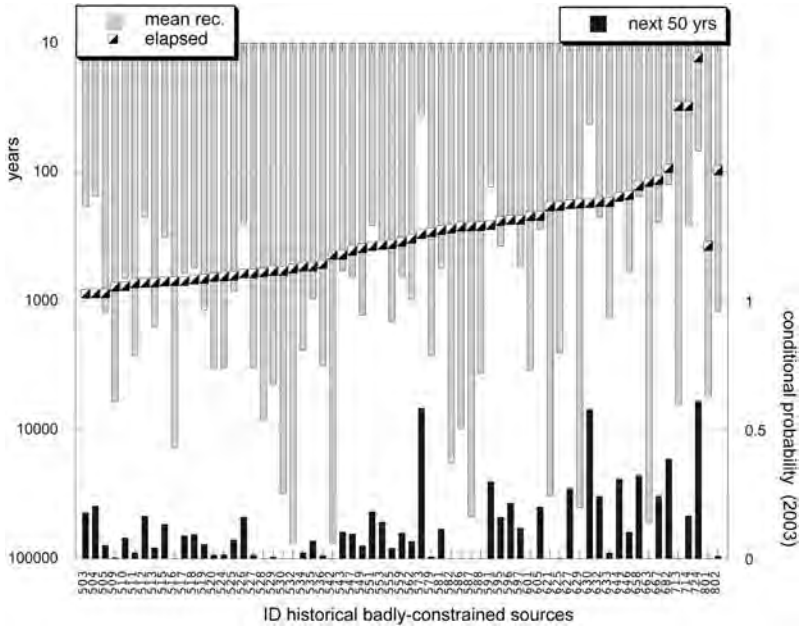

Fig. 19 - Renewal process modelled for DISS historical badly-constrained sources: conditional probability in the next 50 years from 2003 (black bars, right y-axis), given the mean recurrence (grey bars) and elapsed time (squares) reported in the upper part of the graph (left y-axis): the α value is fixed, a priori, equal to 1.

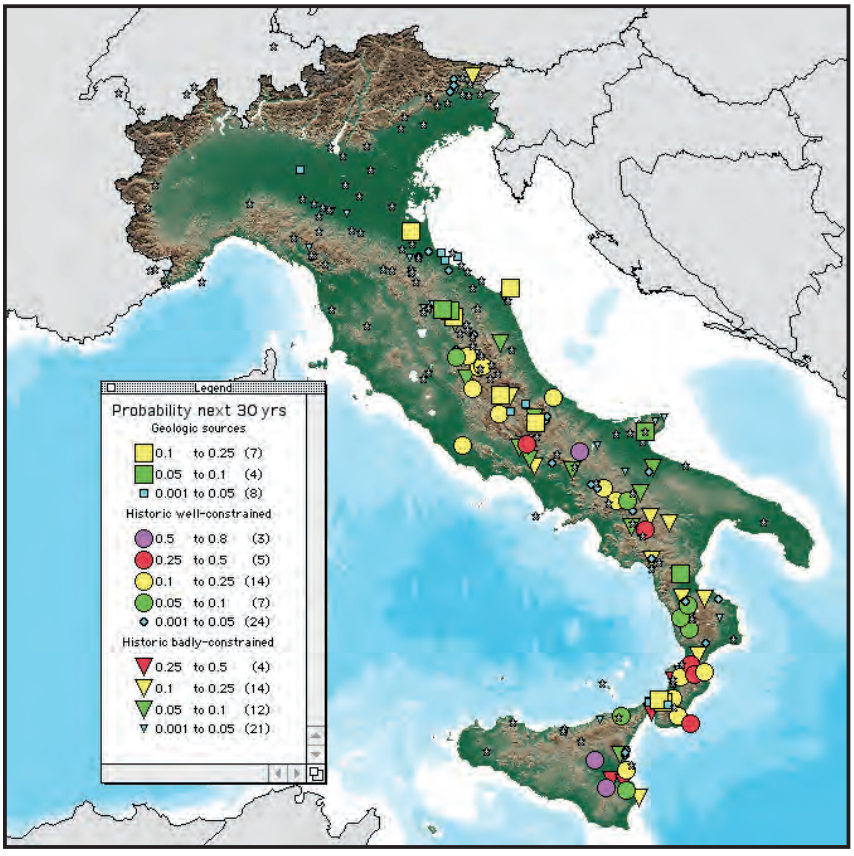

Fig. 20 - Map of the probability of occurrence of a characteristic event on individual DISS' sources (see Fig. 1) in the next 30 years from 2003; small stars for sources having a negligible probability.

of the last event: the last occurrence has been fixed arbitrarily at 3000 B.C. (5000 years of elapsed time) to have a term of comparison with the other sources. The combination of the values of mean recurrence time, elapsed time and α values (fixed values for the historical sources, and variable values for the geological sources, like previously explained) makes the probability of occurrence in the forthcoming years vary strongly, reaching the highest values for moderate earthquakes (M<5.5). 8 sources actually have a conditional probability of a characteristic earthquake in the next 50 years greater than 50%, and they are located in Sicily (ID n. 241 eastern Sicily earthquake, last event in 1718; n. 270 Iblei earthquake, last event in 1818; n. 724 southeastern Sicily earthquake, in 1990; n. 573 Vizzini earthquake, in 1698), Calabria (ID n. 350 Calabria earthquake, in 1978; n. 630 Palmi earthquake, in 1828), and in the Southern Apennines (ID n. 302 Campobasso earthquake, in 1885; n. 296, Meta Mountains earthquake, in 1873).

Finally, the conditional probabilities in the next 30 years (2004-2033) are mapped in Fig. 20, for the whole country, and in Fig. 21 for southern Italy. Different symbols indicate the different kinds of sources (see Fig. 1); only probabilities higher than 0.1% have been mapped.

These maps enhance the contribution of moderate events having relatively short return times, with respect to the sources of large events, which are supposed to have a mean return time usually

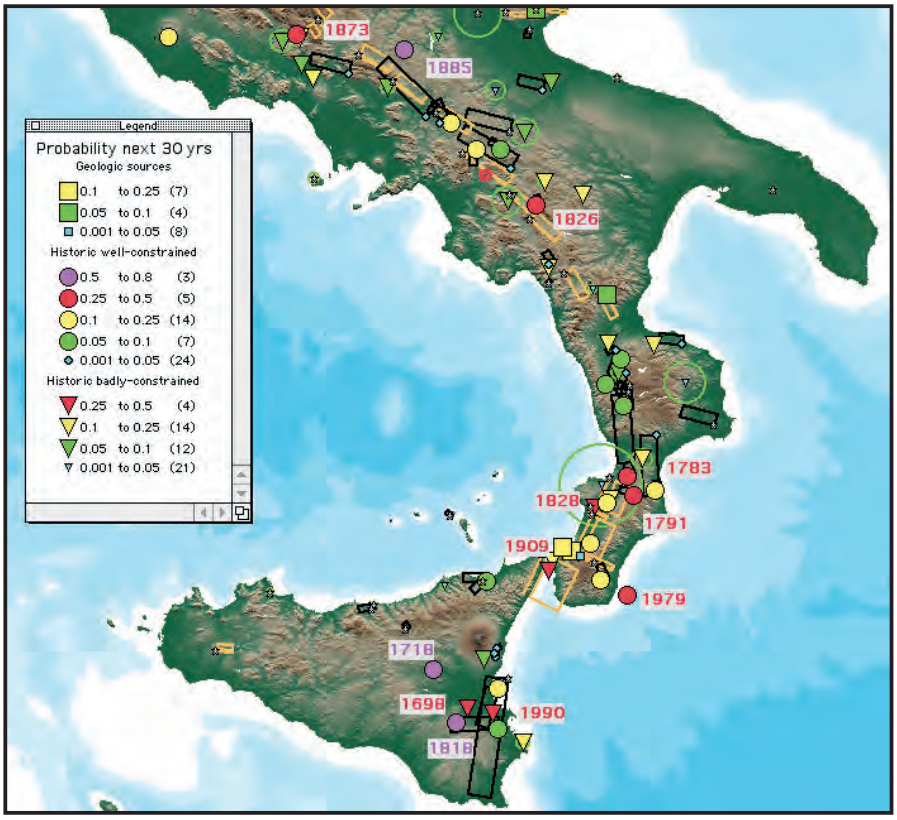

Fig. 21 - Blow-up of Fig. 20 for southern Italy: sources having a probability higher than 25% are labelled with the date of the last earthquake.

much longer than the time elapsed since the last event.

A more reliable definition of the year of occurrences of the geological sources that do not have the date of the last event, and a more accurate choice of mean recurrence time and α values for the historical sources may significantly improve the confidence in these results.

5. Seismic hazard maps

As the initial purpose of the GNDT project was to produce time-dependent seismic hazard maps, I used the geometry and seismicity rates previously obtained to perform a complete seismic hazard assessment. The computations were performed using the well known code SEISRISK III (Bender and Perkins, 1987) on a grid spacing 0.2°, using the attenuation relationships proposed by Ambraseys *et al.* (1996): these relations are based on empirical regressions of European strong-motion data, and have been widely used (e.g. Slejko *et al.*, 1998; Albarello *et al.*, 2000), so that the results obtained here are directly comparable with the previous analyses [see Pace *et al.* (2006) for additional comments on the downward extension of the attenuation model]. The results are expressed in peak ground acceleration (PGA) not expected to be exceeded with a probability of

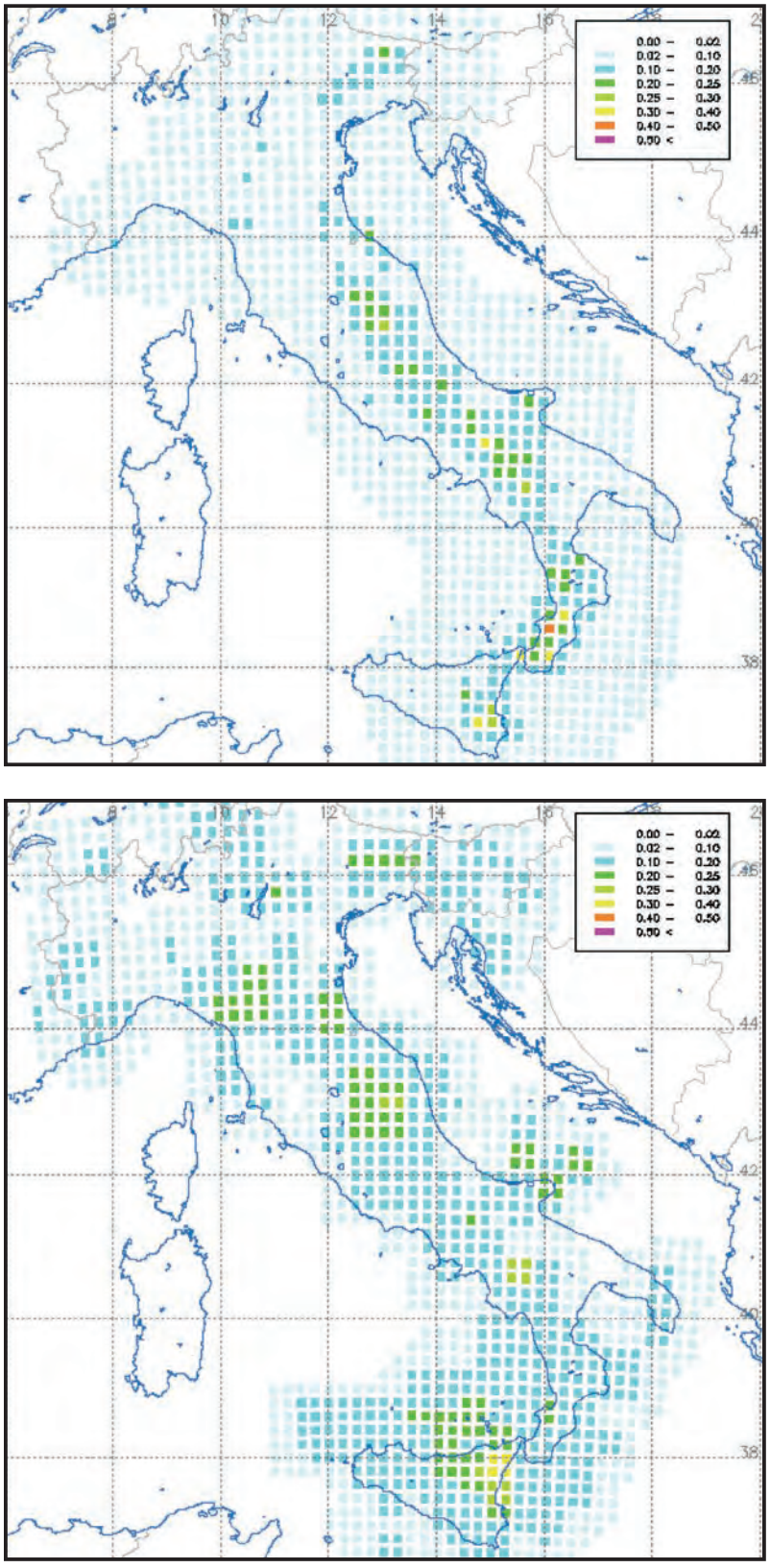

Fig. 22 - Seismic hazard map of the partial models: individual characteristic sources alone (a), background seismicity only (b). Values are PGA (in g) with exceedence probability of 10% in 50 years under Poisson conditions, using the Ambraseys *et al.* (1996) relationship with standard deviation in attenuation.

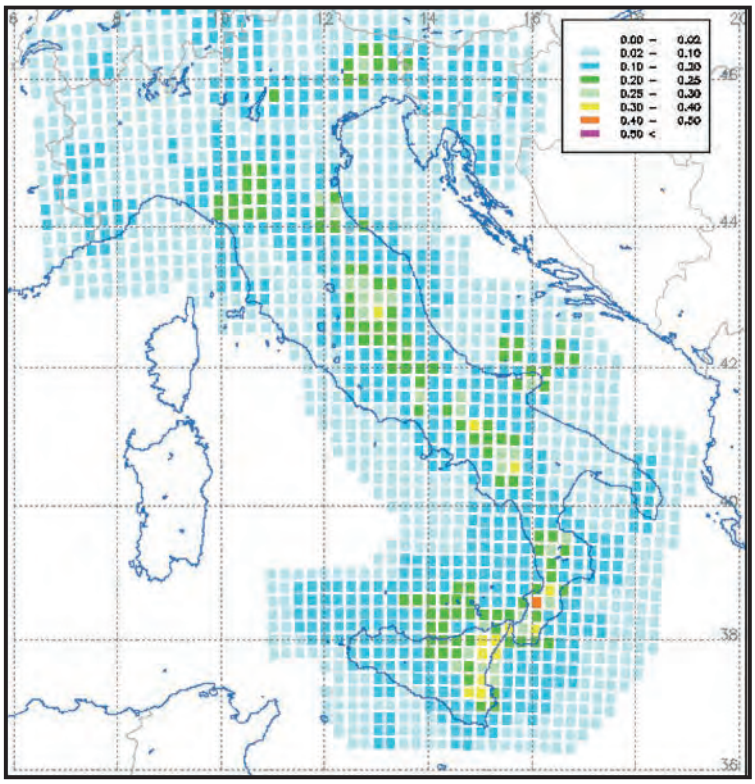

Fig. 23 - Seismic hazard map of the Poissonian model: the partial results of Fig. 22 are integrated by a specific option of the computer code (run continuation). Values are PGA (in g) with exceedence probability of 10% in 50 years.

90% in 10, 30 and 50 years.

Individual sources and background sources constitute different layers of information, run independently and cumulated in the final computations.

The geometry of all the individual sources is consistent with the indications given in the DISS database and the seismicity rate reflects the behaviour of the characteristic event model (Gaussian distribution peaked on mean recurrence time and maximum magnitude, scaled according to the conservation of the seismic moment): their characterization differs for the different kind of sources (geological or historical) as it has been previously described.

The background seismicity, on the contrary, is defined by regular adjacent cell sources, characterized by a G-R distribution in the $2.5<M\leq5.0$ range. The parameters of the G-R relationships derive from the analyses of the instrumental catalogue of the last two decades, previously declustered to satisfy the requisites of independency of the events.

The maps of these two different ingredients are reported in Fig. 22. Results are those that refer to a 90% probability of non-exceedence in 50 years, the standard deviation in the attenuation is included. PGA is represented by quite large, irregular intervals, roughly corresponding to the degrees of the macroseismic intensity scale (Decanini *et al.*, 1995): the pale blue colour, for PGA < 0.1 g may be approximately considered the threshold of no damage. Surprisingly, the low-level seismicity rates derived from the instrumental, short lasting observations, contribute to the hazard,

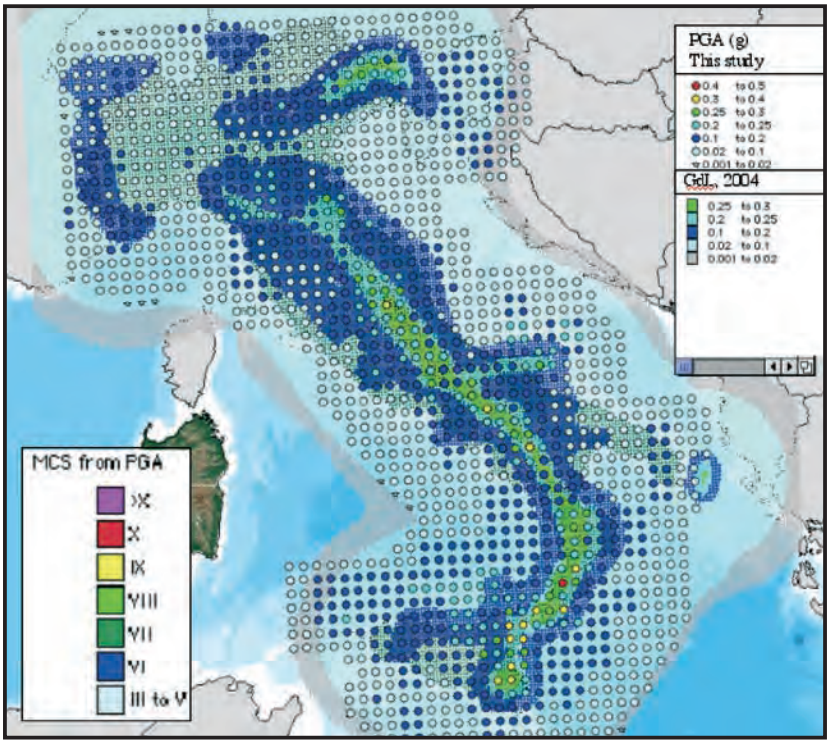

Fig. 24 - Comparison of hazard results: small adjacent coloured squares are the grid of computation used by the Gruppo di Lavoro (2004); large dots are those obtained in this study (see Fig. 23). The equivalence of the macroseismic degrees of the MCS scale with PGA intervals (colours of the symbols) is only indicative.

both in known and in poorly known seismic regions: in fact, the rate of activity located offshore is considerable, even if it is common practice to map the PGA results only on land.

The combination of the two layers of sources gives the results mapped in Fig. 23: the computation is referred to the same stationary hypothesis and return time (T=475) of the most recent maps (Gruppo di Lavoro, 2004). These results are overlapped in Fig. 24 for a visual comparison. Independently of other characteristics of the model (e.g. logic tree, attenuation, etc.), the proposed hazard maps peak the maximum shakings in more restricted areas, and raise the expected shakings outside some well known seismic zones. These effects are essentially due to the use of individual sources (representative of faults) and to the background seismicity derived independently from any seismotectonic model.

The last issue was to introduce the time dependence into the seismic hazard assessment which I did by means of an artefact. The mean recurrence time of the individual sources (and therefore, the annual rate of the characteristic event) is re-computed by imposing that the conditional probability of having an event in the next years (P_{Tdep}) as being equal to the probability of a Poisson process (P_{Pois}) in the same time interval, using the formula:

$$P_{\mathrm{Tdep}} = P_{\mathrm{Pois}} = 1 - e^{-t/T\mathrm{eq}}, \tag{9}$$

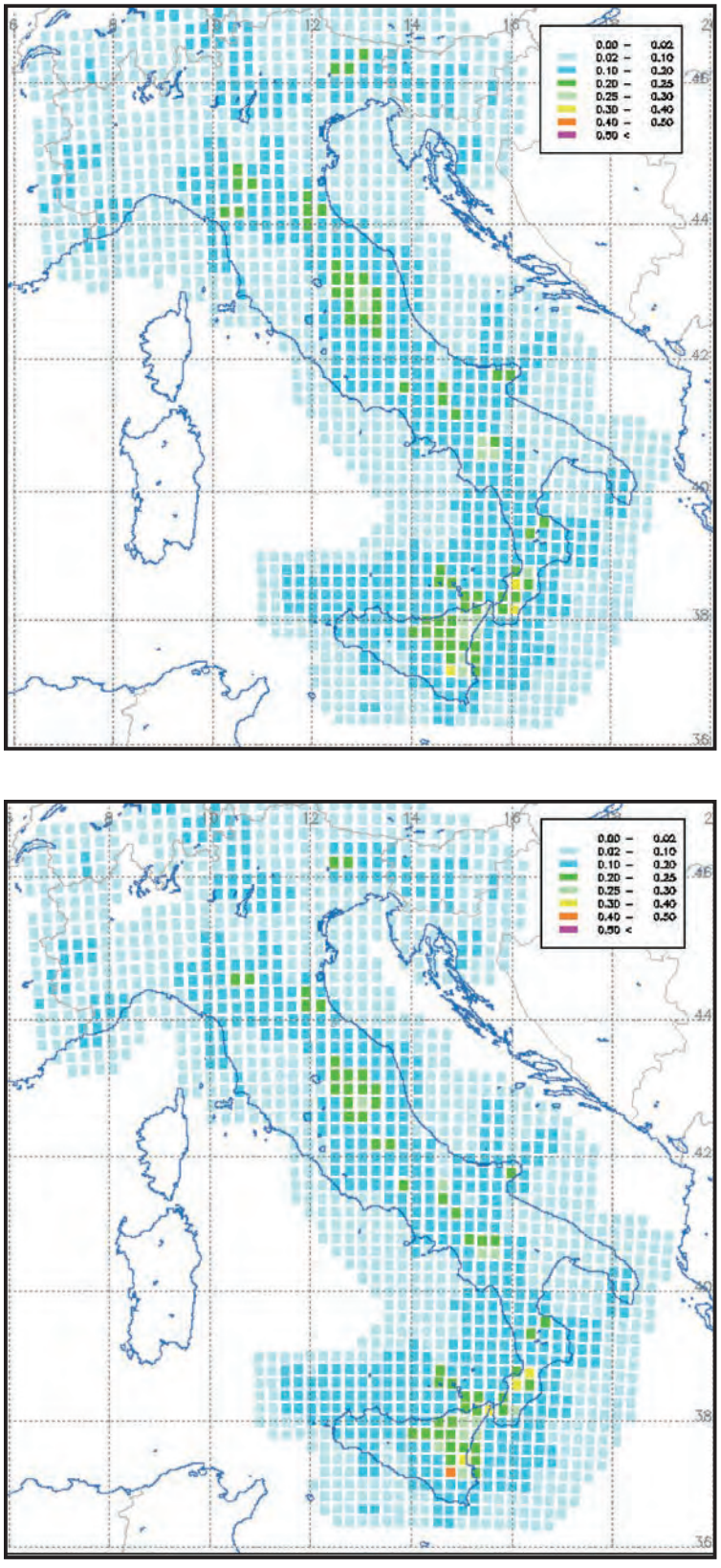

Fig. 25 - Seismic hazard maps of the integrated model, referring to 30 years: (a) results referring to stationary conditions (Poisson); (b) time-dependent results obtained for the next 30 years from 2003, using equivalent fictitious seismicity rates. Values are PGA (in g) with exceedence probability of 10%.

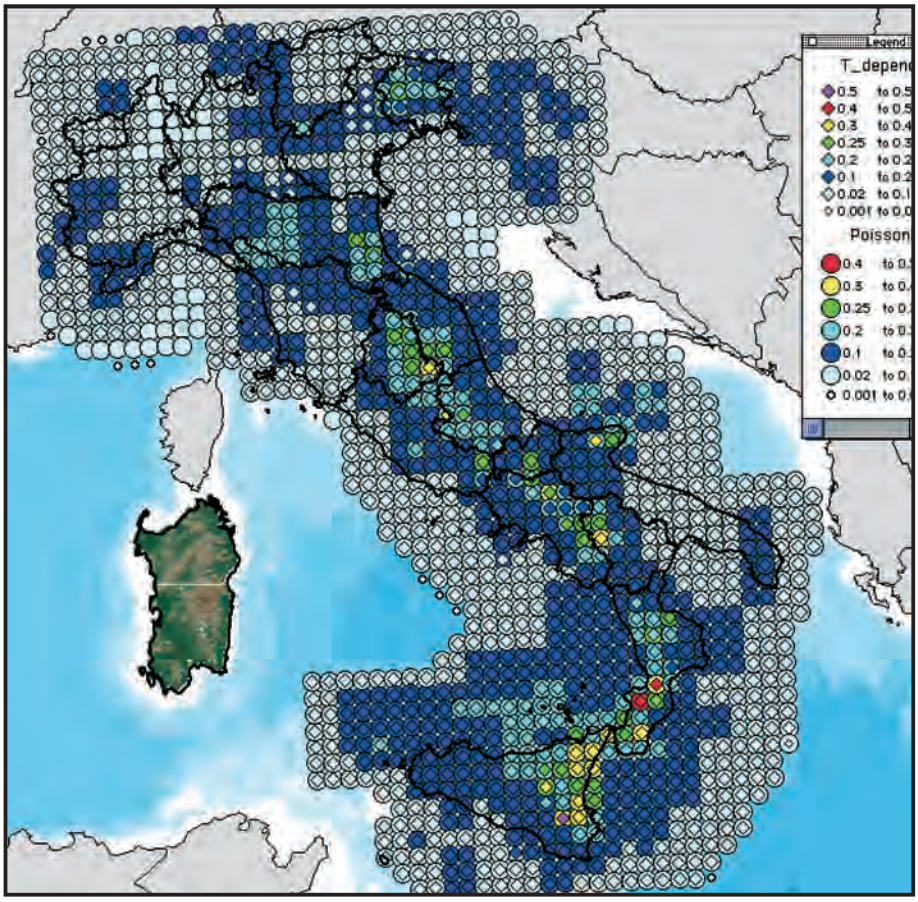

Fig. 26 - Comparison of time-dependent and time-independent hazard results. PGA (in g) with exceedence probability of 10% in 50-year observation period (same as Fig. 23): the differences are appreciable if there is a change of the class represented by colours. The equivalence of the macroseismic degrees of the MCS scale with PGA intervals (colours of the symbols) is only indicative (see the caption of Fig. 27).

where T_{eq} is the fictitious recurrence time, and P_{Tdep} is the conditional probability obtained by the BPT model, in the period of interest (t equal to 10, 30 and 50 years). This simplification, firstly proposed by Wu *et al.* (1995), permits us to introduce equivalent fictitious seismicity rates into traditional seismic-hazard codes, with an accuracy that is acceptable for engineering purposes.

The results may be therefore interpreted as the PGA values, not expected to be exceeded in the next t years from 2003 (year used to compute the elapsed times).

Fig. 25 shows the Poisson and time-dependent results referring to 30 years; Fig. 26 compares the differences obtained on 50 years. Even if the colour classes represent quite large ranges of PGA values, and the differences are limited to some areas, the introduction of time-dependence significantly decreases the hazard in some limited portions of the territory while it increases in some others.

Finally, the results have been aggregated following the administrative boundaries of the

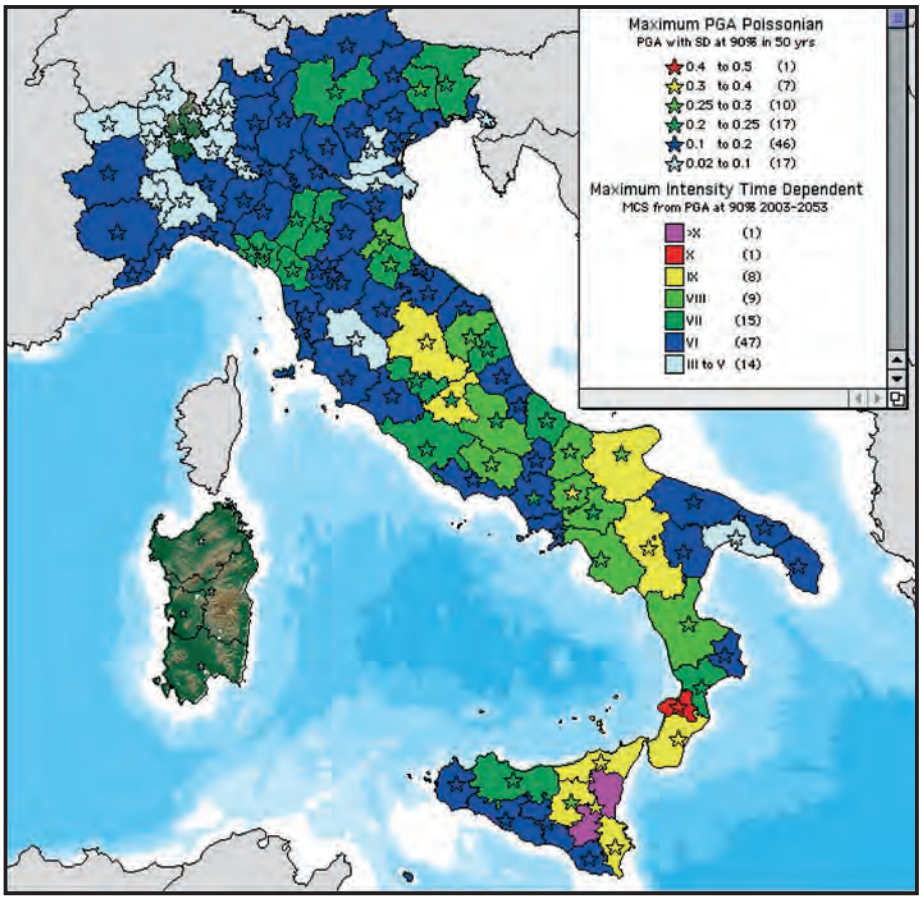

Fig. 27 - Aggregation of the seismic hazard results on the limits of administrative provinces: the maximum value of the nodes inside a province is mapped, for time-dependent (full colour of the area) and time-independent (stars) approaches. The PGA values refer to the non-exceedence probability of 90% in a 50-year observation period.

provinces, mapping the maximum value of the grid nodes falling inside their territory, following the Poisson and time-dependent approaches: to have a more intuitive description of the shakings, PGAs have been considered equivalent to macroseismic intensities, following the legend in Fig. 27. Some provinces show a favourable situation while others expect more seismic hazard, if time-dependent issues are considered.

These analyses have to be considered a preliminary, rough and tentative approximation to the problem of determining the priorities in seismic risk mitigation.

6. Conclusions

The seismogenic source model developed in the frame of the GNDT project named "Probable earthquakes in Italy from the year 2000 to 2030: guidelines for determining priorities in seismic risk mitigation" (Amato and Selvaggi, 2004) is a first test to introduce individual sources and time-dependency to the national scale seismic hazard assessment. Starting from the sources defined by

the Database of Italy's Seismogenic Sources (Valensise and Pantosti, 2001), I derived some of the ingredients needed to characterize the seismicity occurrences of an individual source, and their possible behaviour when treating them as a renewal process. These quantities are essentially: 1) the magnitude of the maximum earthquake that is treated like a characteristic event; 2) the uncertainty in magnitude estimate that is used to shape a Gaussian distribution; 3) the mean recurrence time, associated to the characteristic event that is used to fix the annual number of events of the Gaussian distribution; 4) the uncertainty in mean recurrence times that is used to fix the periodicity characteristics of the BPT distributions, used for modelling the renewal process.

Then, I characterized the so-called background seismicity with an independent elaboration of the instrumental catalogue of Italian earthquakes. After a filtering processing of the catalogue, capable of obtaining a subset of independent events, the *a*- and *b*-values of the G-R relationship have been computed by lsq regression on experimental data in a 20 km distance from the nodes of a grid; the *a*-values are normalized to time and area units. The nodes having an acceptable dataset for the G-R interpolation (at least 5 events) have been therefore used as centre of regular source cells whose seismicity rates are shaped by the G-R relation, in the magnitude range 2.5-5.0.

This information permits us to compute: a) the probability of occurrence of a characteristic event conditional to the time of the last event for all the individual sources (Fig. 20); b) the expected shakings both under Poisson and non-Poisson assumptions (Figs. 23, 25 and 26).

As some arbitrary assumptions have been made to fill the lack of experimental data, the results obtained must be considered mainly for their methodological approach to the problem and their application to seismic protection strategies needs to be done with great caution.

Acknowledgements. I wish to thank R. Console and D. Slejko for their detailed comments that improved the paper considerably and enabled me to avoid some pitfalls of the first version. The study was supported by INGV-GNDT funds of the Project "Terremoti probabili in Italia tra l'anno 2000 e il 2030: elementi per la definizione di priorità degli interventi di riduzione del rischio sismico" coordinated by A. Amato and G. Selvaggi. The final results released by this study may be found in the "Prodotto N.14" at the web site address http://gndt.ingv.it/Att_scient/Prodotti_consegnati/Amato_Selvaggi/prodotti_Amato.htm.

REFERENCES

Aki K.; 1965: *Maximum likelihood estimate of b in the formula logN=a-bM and its confidence limits*. Bull. Earth. Res. Inst., **43**, 237-239.

Albarello D., Bosi V., Bramerini F., Lucantoni A., Naso G., Peruzza L., Rebez A., Sabetta F. and Slejko D.; 2000: *Carte di pericolosità sismica del territorio nazionale.* Quaderni di Geofisica, **12**, 1-7.

Amato A., and Selvaggi G.; 2004: *Terremoti probabili in Italia tra l'anno 2000 e il 2030: elementi per la definizione di priorità degli interventi di riduzione del rischio sismico.* In: GNDT (ed), Scientific Reports - 3rd year of activities, URL: http://gndt.ingv.it/Att_scient/PE2002_Brief_Reports/brief_reports_con_int.htm.

Ambraseys N. N., Simpson K. A. and Bommer J. J.; 1996: *Prediction of horizontal response spectra in Europe.* Earth. Eng. Struct. Dyn., **25**, 371-400.

Bender B., and Perkins D. M.; 1987: *SEISRISK III; a computer program for seismic hazard estimation.* U. S. Geological Survey Bulletin 1772, 48 pp., URL: http://earthquake.usgs.gov/research/hazmaps/publications/Legacy_Code/version.php

Castello B., Selvaggi G., Chiarabba C. and Amato A.; 2005: *CSI Catalogo della sismicità italiana 1981-2002, v. 1.0*. INGV-CNT, Rome, URL: http://www.ingv.it/CSI/.

Chiarabba C.; 2003: *CATA_MAg81-02.01 Catalogo strumentale dei terremoti italiani dal 1981 al 2002.* Internal File Report, INGV, Rome.

Decanini L., Gavarini C. and Mollaioli F.; 1995: *Proposta di definizione delle relazioni tra intensità macrosismica e parametri del moto del suolo.* In: Conference Proceedings L'ingegneria sismica in Italia, pp. 63-72.

Ellsworth W. L., Matthews M. V., Nadeau R. M., Nishenko S. P., Reasenberg P.A. and Simpson R. W.; 1999: *A physically-based earthquake recurrence model for estimation of long-term earthquake probabilities.* U. S. Geological Survey, Open-File Report, 99-522, 22 pp.

Faenza L., Marzocchi W. and Boschi E.; 2003: *A non-parametric hazard model to characterize the spatio-temporal occurrence of large earthquakes; an application to the Italian catalogue.* Geophys. J. Int., **155**, 521-531.

Field E. H., Johnson D. D. and. Dolan J. F; 1999: *A mutually consistent seismic-hazard source model for Southern California.* Bull. Seism. Soc. Am., **89**, 559-578.

Gruppo di Lavoro; 1999: *Proposta di riclassificazione sismica del territorio nazionale.* Ingegn. Sismica, **14**, 5-14.

Gruppo di Lavoro; 2004: *Redazione della mappa di pericolosità sismica prevista dall'Ordinanza PCM 3274 del 30 marzo 2003.* Rapporto conclusivo per il Dipartimento di Protezione Civile. INGV, Milano-Roma, 65 pp.

Gruppo di Lavoro Scuotibilità; 1979: *Carte preliminari di scuotibilità del territorio nazionale.* Esa, Roma, CNR PF Geodinamica.

Hanks T. C. and Kanamori H.; 1979: *A moment magnitude scale.* J. Geoph. Res., **84**, 2348-2350.

Kagan Y. Y. and Jackson D. D.; 1993: *Seismic gap hypothesis: ten years after.* J. Geophys. Res., **98**, 419-431.

Knopoff L.; 2000: *The magnitude distribution of declustered earthquakes in Southern California.* Proc. Natl. Acad. Sci. USA, **97**, 11880-11884.

Margottini C., Ambraseys N.N. and Screpanti A.; 1993: *La magnitudo dei terremoti italiani del XX secolo.* Technical report, ENEA, Roma, 57 pp. Earth. Eng. Struct. Dyn., **22**, 1017-1030.

Marzocchi W., Sandri L. and Boschi E.; 2003: *On a validation of earthquake-forecasting models: the case of pattern recognition algorithms.* Bull. Seism. Soc. Am., **93**, 1994-2004.

Matthews M. V., Ellsworth W. L. and Reasenberg P. A.; 2002: *A Brownian model for recurrent earthquakes.* Bull. Seism. Soc. Am., **92**, 2233-2250.

Michetti A. M., Ferreli L., Serva L. and Vittori E.; 1997: *Geological evidence for strong historical earthquakes in an "aseismic" region; the Pollino case (southern Italy).* In: Hancock P. and Michetti A. (eds), Paleoseismology; understanding past earthquakes using Quaternary geology, Journal of Geodynamics, **24**, 67-86.

Muir Wood R.; 1993: *From global seismotectonics to global seismic hazard.* In: Giardini D. and Basham P. (eds), Technical planning volume of the ILP's Global seismic hazard assessment program for the UN/ IDNDR including the Proceedings of the GSHAP technical planning meeting, Annali di Geofisica, **36**, 153-168.

Pace B., Peruzza L., Lavecchia G. and Boncio P.; 2006: *Layered seismogenic source model and probabilistic seismic hazard analyses in central Italy.* Bull. Seism. Soc. Am., **96**, 107-132.

Peruzza L. (ed); 1999: *Progetto MISHA. Metodi Innovativi per la Stima dell'HAzard - Applicazione all'Italia Centrale*. CNR - Gruppo Nazionale per la Difesa dai Terremoti, Trieste, Studio Gamma, 176 pp. URL: http:gndt.ingv.it/pubblicazioni/monografiche_ disponibili_con_intestazione.htm.

Peruzza L. and Pace B.; 2002: *Sensitivity analysis for seismic source characteristics to probabilistic seismic hazard assessment in Central Apennines (Abruzzo area).* Boll. Geof. Teor. Appl., **43**, 79-100.

Peruzza, L., Pantosti D., Slejko D. and Valensise L.; 1997: *Testing a new hybrid approach to seismic hazard assessment: an application to the Calabrian Arc (southern Italy).* Natural Hazards, **14,** 113-126.

Petrini V., Bosi C., Bigi G., Eva C., Iaccarino E., Luongo G., Postpischl D., Praturlon A., Riuscetti M., Scandone P., Scarpa R., Stucchi M. and Vezzani L.; 1980: *Proposta di riclassificazione sismica del territorio nazionale.* Progetto Finalizzato Geodinamica, Rome, ESA, 83 pp.

Postpischl D.; 1985: *Catalogo dei terremoti italiani dal 1000 al 1980.* Quaderni della Ricerca Scientifica, Roma, 114 pp.

Romeo R.; 2005: *Earthquake hazard in Italy, 2001-2030.* Nat. Haz., **36**, 383-405.

Schwartz D. P. and Coppersmith K. J.; 1984: *Fault behaviour and characteristic earthquakes; examples from the Wasatch and San Andreas fault zones.* Journal of Geophysical Research, **89**, 5681-5698.

Selvaggi G.; 1998: *Spatial distribution of horizontal seismic strain in the Apennines from historical earthquakes.* Ann.

Geof., **41**, 241-251.

Slejko D., Peruzza L. and Rebez A.; 1998: *Seismic hazard maps of Italy.* Ann. Geof., **41**, 183-214.

Sornette D. and Knopoff L.; 1997: *The paradox of the expected time until the next earthquake.* Bull. Seism. Soc. Am., **87**, 789-798.

Stucchi M. and Albini P.; 2000: *Quanti terremoti distruttivi abbiamo perso nell'ultimo millennio? Spunti per la definizione di un approccio storico alla valutazione della completezza.* In: Galadini F., Meletti C. and Rebez A. (eds), Le ricerche del GNDT nel campo della pericolosità sismica (1996-1999), CNR-Gruppo Nazionale per la Difesa dai Terremoti, Roma, pp. 333-343.

Utsu T.; 1965: *A method for determining the value of b in the formula logN=a-bM showing the magnitude-frequency relation for earthquakes.* Geophysical Bulletin Hokkaido University, **13**, 99-103.

Utsu T.; 1966: *A statistical significance test of the difference in b-value between two earthquake groups.* Journal Physics Earth, **14**, 37-40.

Valensise G. and Pantosti D. (eds); 2001: *Database of potential sources for earthquakes larger than M 5.5 in Italy.* Ann. Geof., Suppl. to **44(4)**, 180 pp, CD-Rom.

Weichert D. H.; 1980: *Estimation of the earthquake recurrence parameters for unequal observation periods for different magnitudes.* Bull. Seism. Soc. Am., **70**, 1337-1346.

Wells D. L. and Coppersmith K. J.; 1994: *New empirical relationships among magnitude, rupture length, rupture width, rupture area, and surface displacement.* Bull. Seism. Soc. Am., **84**, 974-1002.

Working Group CPTI; 2004: *Catalogo Parametrico dei Terremoti Italiani, versione 2004 (CPTI04).* INGV, Bologna, URL: http://emidius.mi.ingv.it/CPTI/home.html.

Working Group on California Earthquake Probabilities; 1999: *Earthquake probabilities in the San Francisco Bay region; 2000 to 2030, a summary of findings.* U. S. Geological Survey, Open-File Report 99-517, 60 pp.

Working Group on California Earthquake Probabilities; 2003: *Earthquake probabilities in the San Francisco Bay region; 2002 to 2031.* U. S. Geological Survey, Open-File Report 03-214, 234 pp.

Wu S. C., Cornell C. A. and Winterstein S. R.; 1995: *A hybrid recurrence model and its implication on seismic hazard results.* Bull. Seism. Soc. Am., **85,** 1-16.

Youngs R. R., and Coppersmith K. J.; 1985: *Implications of fault slip rates and earthquake recurrence models to probabilistic seismic hazard estimates.* Bull. Seism. Soc. Am., **75,** 939-964.

Corresponding author: Laura Peruzza
Istituto Nazionale di Oceanografia e Geofisica Sperimentale
Borgo Grotta Gigante 42/c, 34010 Sgonico (TS) Italy
e-mail: lperuzza@inogs.it, phone +39 0402140244